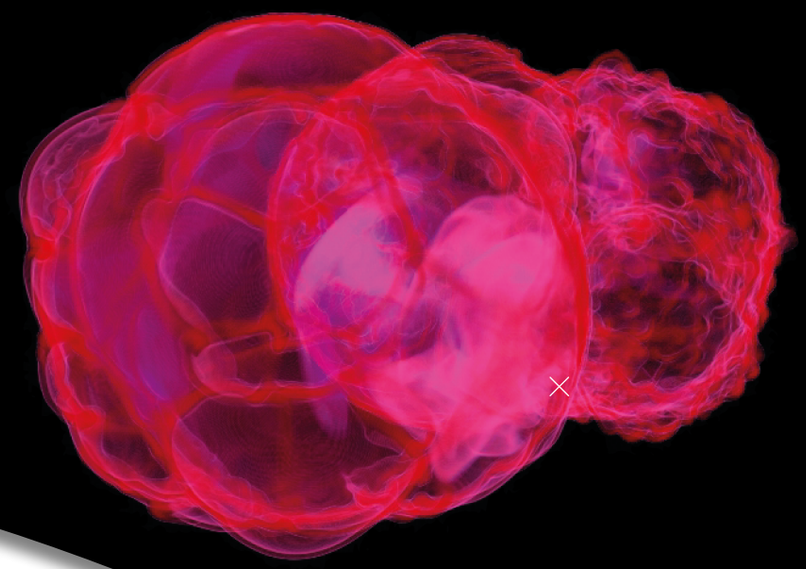

Simulations of the Local Superbubble

Michael M. Schulreich

In collaboration with:
Dieter Breitschwerdt (TU Berlin)
Jenny Feige (TU Berlin)
Christian Dettbarn (ARI Heidelberg)
Miguel de Avillez (U Évora)

12 December 2018 :: Searching for the sources of Galactic cosmic rays :: APC, Paris

North Pacific Ocean

Recovery of the ferromanganese (FeMn) crust sample 237KD from the equatorial Pacific floor in 1976

Image credits: Google Maps (background), http://www.oceanexplorer.noaa.gov (top right photo), D. Quadfasel (all other photos)

South Pacific Ocean

Relics of a *Blast from the Past*?

- Each crust layer corresponds to certain age range
- Knie+ (2004) detected significant abundance increase of radioisotope ^{60}Fe in ~2.2 Myr-old layer; signal confirmed by Fitoussi+ (2008)

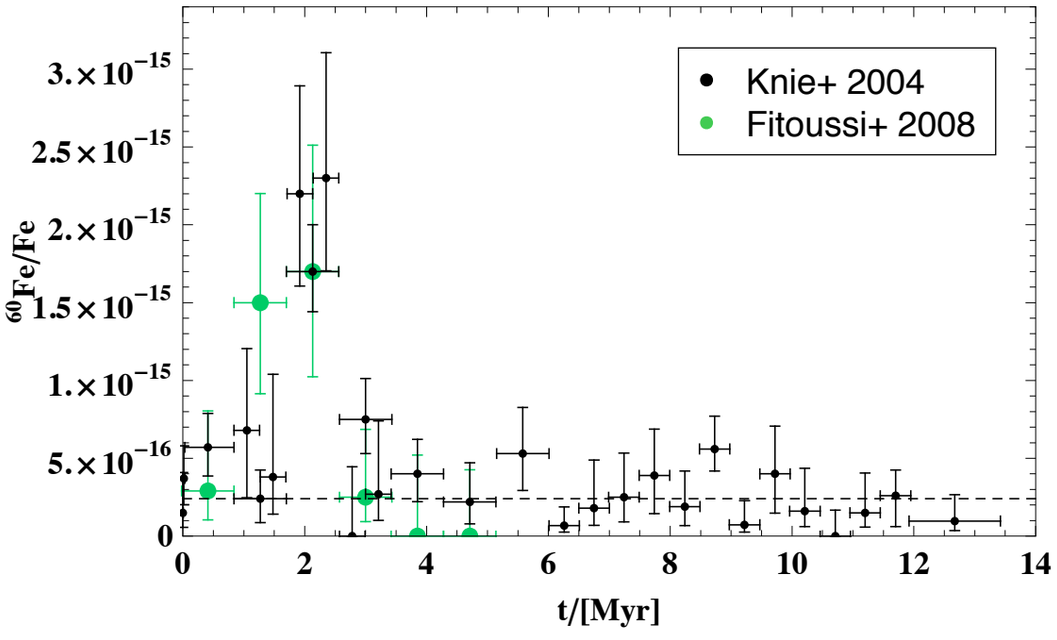

What's so special about ^{60}Fe?

- Produced during late shell-burning phase in massive stars; predominantly released by core-collapse/electron-capture SNe (cf. Knödlseder+ 2004)
- Low terrestrial background
- Comparatively long half-life ($t_{1/2}$ ~ 2.62 Myr) allows for extensive ISM traveling → detectable by β^- decay via ^{60}Co and ɣ-ray emission at 1173 and 1333 keV (Wang+ 2007)

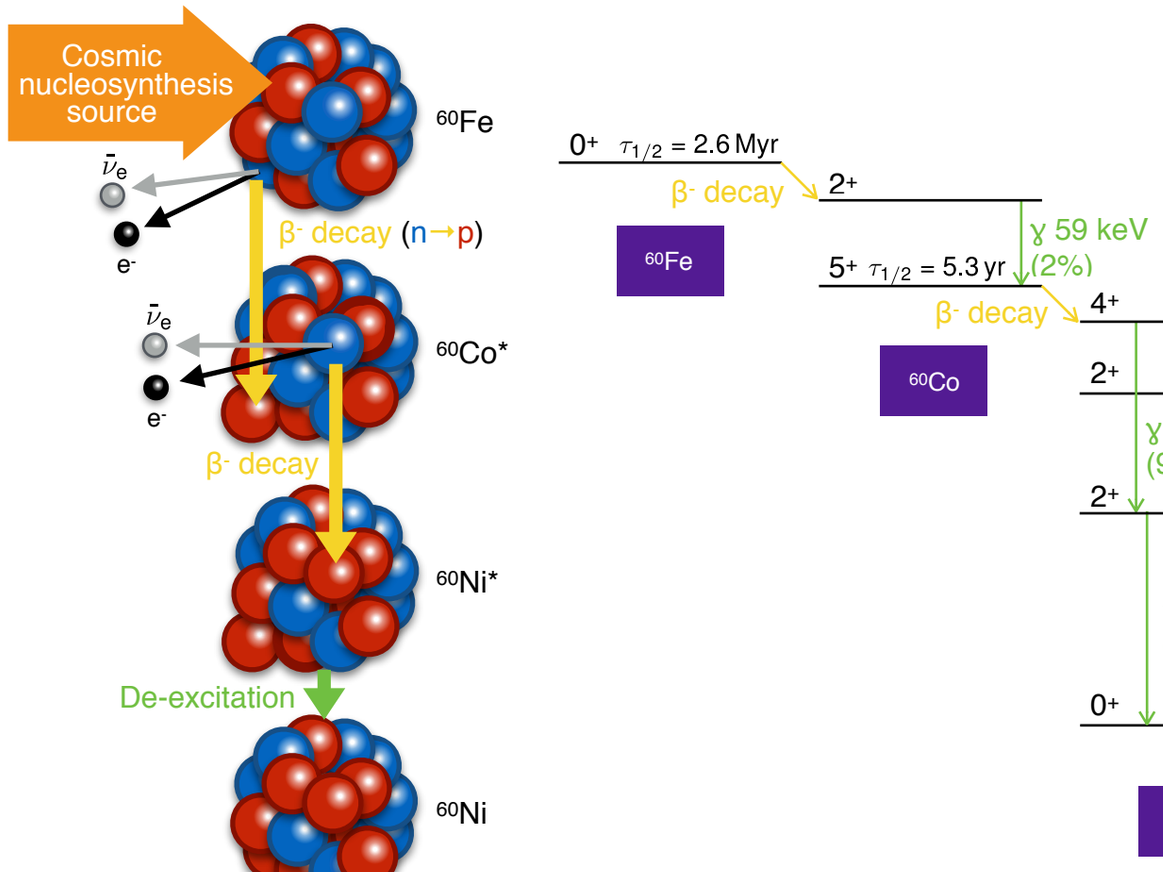

- Link between the ^{60}Fe anomaly and recent SNe near Earth that also contributed to the formation of the **Local Bubble** (LB)

The discovery of the Local Bubble

- Our Galactic habitat
- Color excess measurements (Fitzgerald 1968)
  - Sun situated in interstellar dust hole (~50×100 pc)
- Sounding rocket flights (McCammon & Sanders 1990): Mappings of diffuse **soft** X-ray background
  - due to energy dependent absorption: plasma must be **local**
- Ly-α absorption from nearby hot star spectra
  - HI deficient hole (10^{-2}–10^{-3} cm^{-3}) → anti-correlation!
  - **Displacement model** (Sanders+ 1977; Snowden+ 1991): hot plasma (~10^6 K) **pushes HI gas away**
- Responsible for ~60% of the 0.25-keV flux in the Galactic plane (Galeazzi+ 2014) → **bold confirmation of its existence**
- Further constraints for the LB dimensions from …
  - ROSAT "shadowing experiments" (hot gas component; Snowden+ 1998)
  - NaI absorption lines toward hundreds of stars with known parallaxes (Sfeir+ 1999, Lallement+ 2003) → R ~ 60–250 pc (in Gal. plane); open towards poles? → local chimney? (Welsh+ 1999)
  - Extinction studies toward 71,000 background stars (Lallement+ 2018); blue/yellow: high/low opacity; shown volume: 4000×4000×600 pc^3

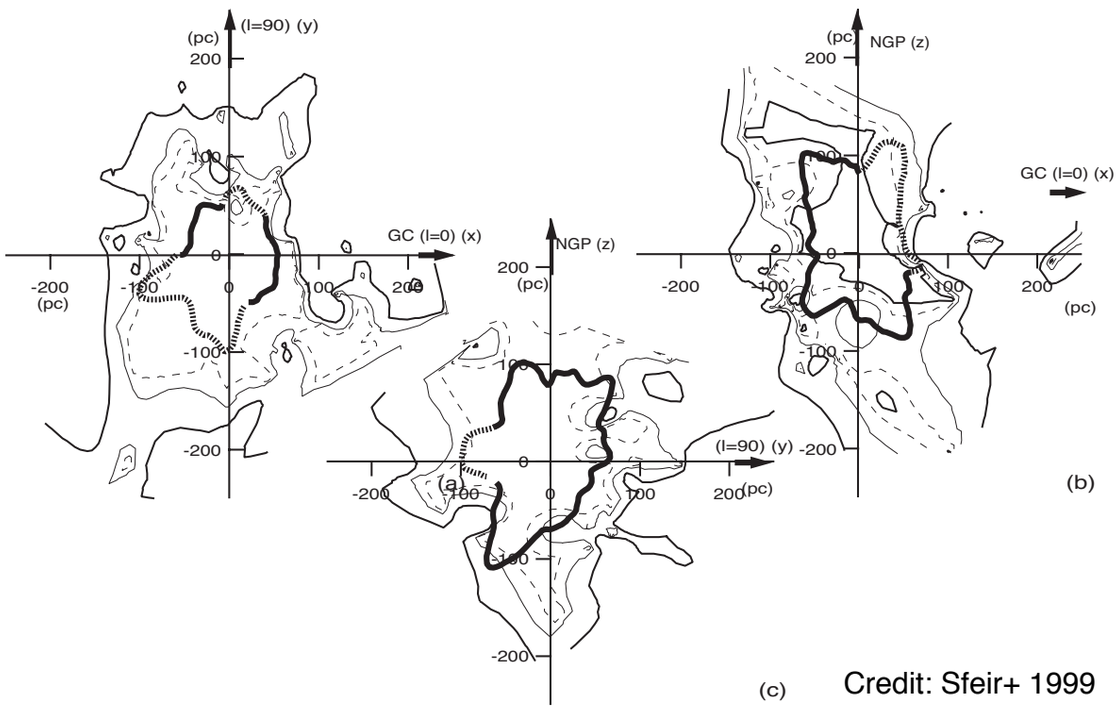

Credit: Sfeir+ 1999

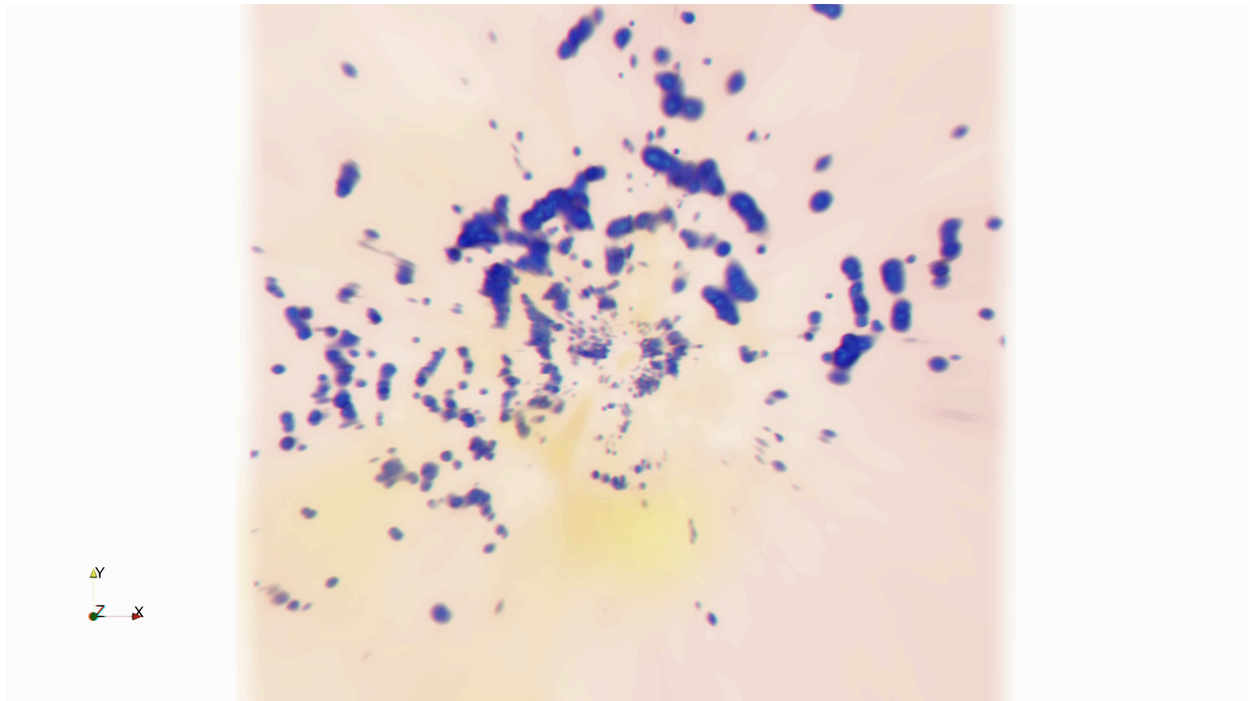

The discovery of the Local Bubble

- Our Galactic habitat
- Color excess measurements (Fitzgerald 1968)
  - Sun situated in interstellar dust hole (~50×100 pc)
- Sounding rocket flights (McCammon & Sanders 1990): Mappings of diffuse **soft** X-ray background
  - due to energy dependent absorption: plasma must be **local**
- Ly-α absorption from nearby hot star spectra
  - HI deficient hole (10^{-2}–10^{-3} cm^{-3}) → anti-correlation!
  - **Displacement model** (Sanders+ 1977; Snowden+ 1991): hot plasma (~10^6 K) **pushes HI gas away**
- Responsible for ~60% of the 0.25-keV flux in the Galactic plane (Galeazzi+ 2014) → **bold confirmation of its existence**
- Further constraints for the LB dimensions from …
  - ROSAT "shadowing experiments" (hot gas component; Snowden+ 1998)
  - NaI absorption lines toward hundreds of stars with known parallaxes (Sfeir+ 1999, Lallement+ 2003) → R ~ 60–250 pc (in Gal. plane); open towards poles? → local chimney? (Welsh+ 1999)
  - Extinction studies toward 71,000 background stars (Lallement+ 2018); blue/yellow: high/low opacity; shown volume: 4000×4000×600 pc^3

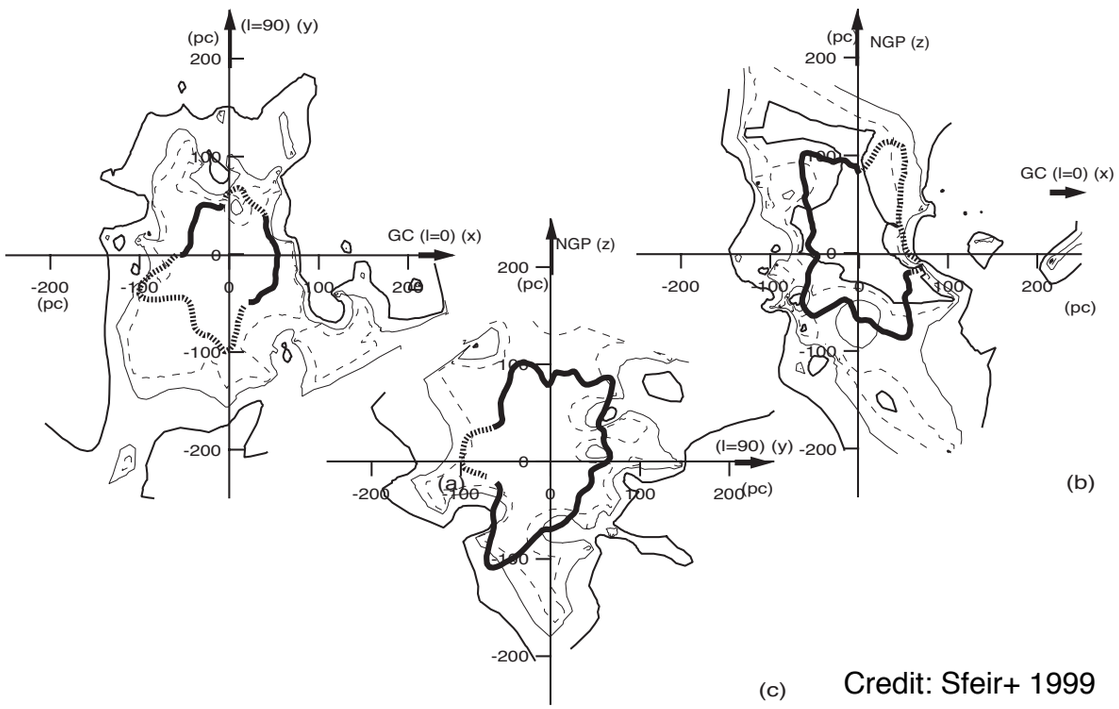

Credit: Sfeir+ 1999

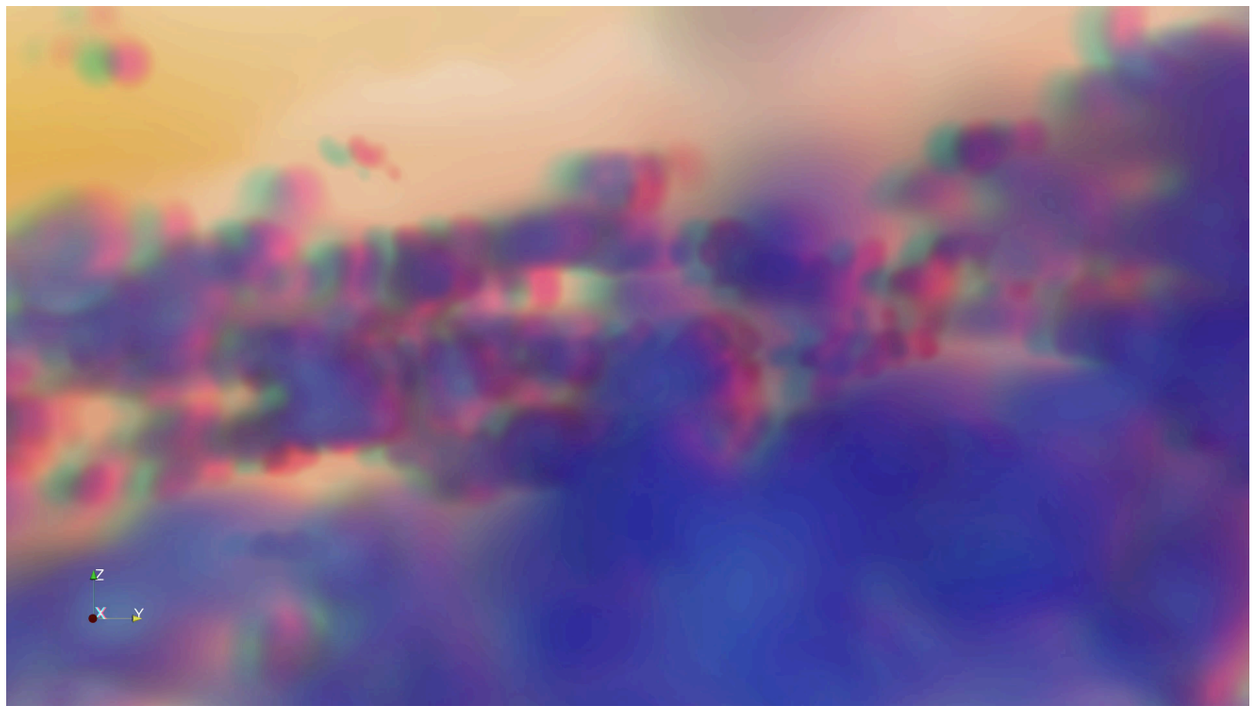

The origin of the Local Bubble

- **Widely accepted origin:** several nearby SN explosions in the last ~10 Myr (e.g., Smith & Cox 2001)
  - But, **no young stellar cluster** could be found inside its boundaries
- Berghöfer & Breitschwerdt (2002) searched for moving group → Pleiades subgroup B1
- Fuchs+ (2004) analyzed vol. complete sample ($D \sim 400$ pc) using HIPPARCOS and ARIVEL (**x**-**p**) phase space data
- Selection criterion: compact in real & vel. space → 79 B stars
- **Cluster age:** compare cluster turn-off point with isochrones (Schaller+ 1992) → $\tau_c \sim 20$–30 Myr
- **COM-trajectory** derived from epicyclic eqs.
- Stars entered LB at $\Delta\tau \sim 10$–15 Myr ago
- **Most probable trajectories:** using Gaussian error distr. in positions and proper motions
- **Number of past SNe:** IMF (1 star per bin!) for young massive stars (Massey+ 1995) → 14–20 SNe exploding inside LB
- **MS lifetime** of SN progenitors: $\tau = 1.6\times10^8\ (M/\mathrm{M}_\odot)^{-0.932}$ yr (for $2 \le M/\mathrm{M}_\odot \le 67$); results from fitting isochrone data
- **Explosion times:** $t_{exp} = \tau - \tau_c$ (assume: coeval star formation)
- Combining most probable trajectories & explosion times → **most probable explosion sites**

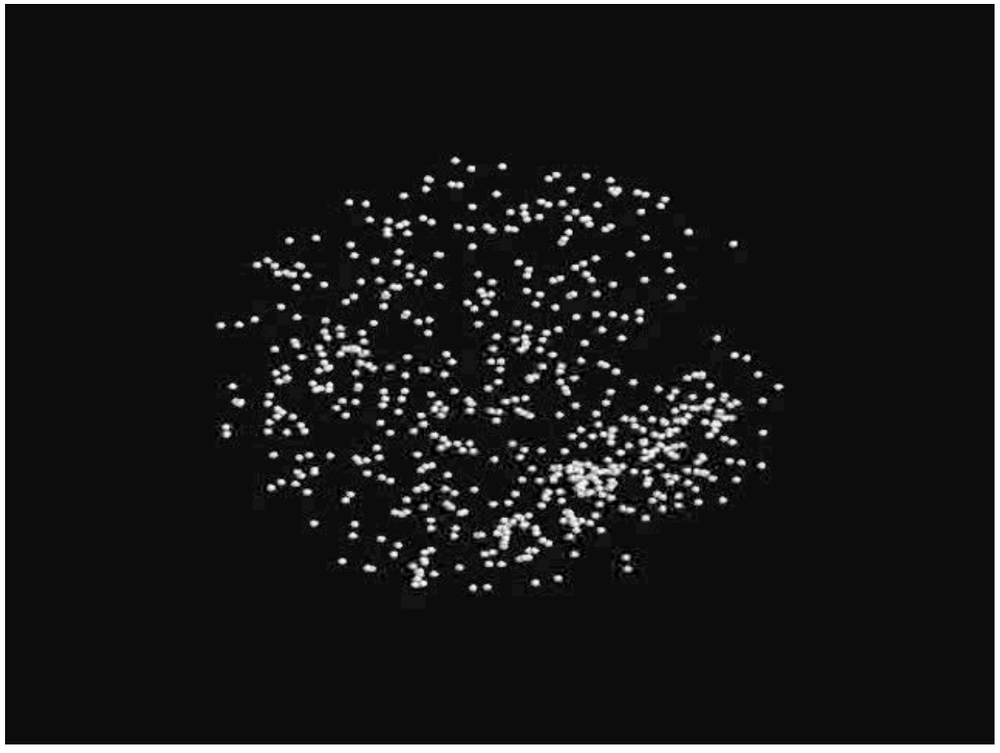

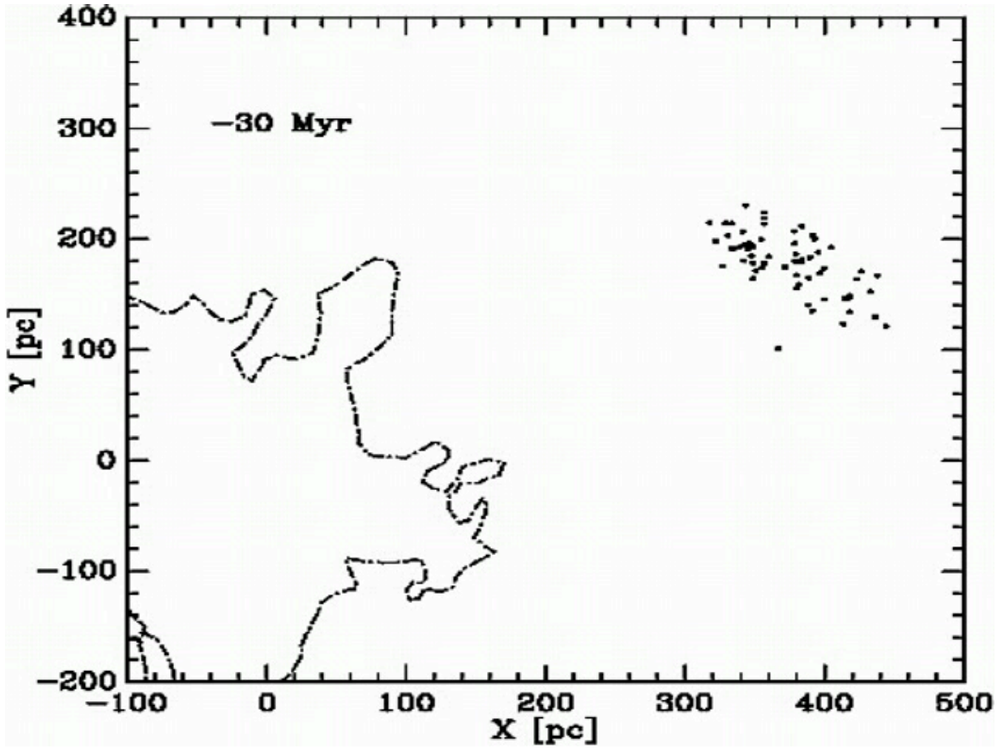

Credit: Fuchs+ (2006)

The origin of the Local Bubble

- **Widely accepted origin:** several nearby SN explosions in the last ~10 Myr (e.g., Smith & Cox 2001)
  - But, **no young stellar cluster** could be found inside its boundaries
- Berghöfer & Breitschwerdt (2002) searched for moving group → Pleiades subgroup B1
- Fuchs+ (2004) analyzed vol. complete sample ($D \sim 400$ pc) using HIPPARCOS and ARIVEL (**x-p**) phase space data
- Selection criterion: compact in real & vel. space → 79 B stars
- **Cluster age:** compare cluster turn-off point with isochrones (Schaller+ 1992) → $\tau_c \sim 20$–30 Myr
- **COM-trajectory** derived from epicyclic eqs.
- Stars entered LB at $\Delta\tau \sim 10$–15 Myr ago
- **Most probable trajectories:** using Gaussian error distr. in positions and proper motions
- **Number of past SNe:** IMF (1 star per bin!) for young massive stars (Massey+ 1995) → 14–20 SNe exploding inside LB
- **MS lifetime** of SN progenitors: $\tau = 1.6\times10^8\ (M/M_\odot)^{-0.932}$ yr (for $2 \le M/M_\odot \le 67$); results from fitting isochrone data
- **Explosion times:** $t_{exp} = \tau - \tau_c$ (assume: coeval star formation)
- Combining most probable trajectories & explosion times → **most probable explosion sites**

Analytical study (Feige 2010; Breitschwerdt+ 2016)**:**

- SNR expansion into previous remnant ($\rho \sim R^{9/2}$) → low Mach-number shocks due to hot interior
- Outer LB shell expansion due to Weaver+ (1977)
- ^{60}Fe content (yield taken from stellar evolution) entrained and deposited by SN blast waves

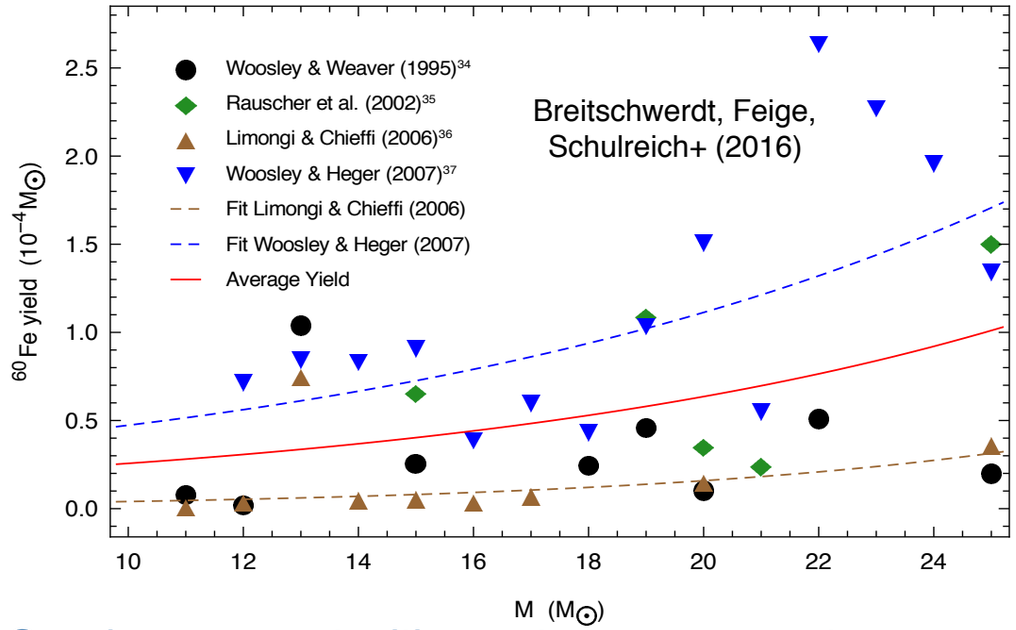

- Good agreement with crust measurements
- Results show that LB SNe can be responsible for ^{60}Fe deposition

Detailed transport modelling in turbulent medium requires

- performing 3D high-res. numerical simulations
- **treating ^{60}Fe as passive scalars**
- using self-consistently evolved turbulent ISM as a typical background medium (like Breitschwerdt & Avillez 2006)

Numerical simulations

Mesoscale ISM simulations using publicly available AMR (magneto-)hydrodynamics and N-body code RAMSES (Teyssier 2002)

- Star formation (IMF; collisionless particles represent massive stars) at Gal. rate
- Feedback from stellar winds and SNe
- Solar wind bubble (heliosphere)
- Self-gravity of the gas & Galactic gravitational potential
- Heating & CIE cooling for gas with solar metallicity (using CLOUDY code)

	Homogeneous background models (A & B)	Inhomogeneous background model (C)
Box size	3 x 3 x 3 kpc^3	3 x 3 x 3 kpc^3
Highest grid resolution	0.7 pc (ℓ_{max} = 12)	2.9 pc (ℓ_{max} = 10)
Boundary conditions (vertical faces / top and bottom)	periodic / periodic	periodic / outflow
Total evolution time	12.6 Myr	192.6 Myr (180 + 12.6 Myr)
Initial gas distribution	homogeneous	analytical fit to observational data of the Galaxy (Ferrière 1998)
External gravitational field	no	yes
Self-gravity	yes	no

Modeling the Loop I superbubble

- Further “boundary condition” …
- ROSAT PSPC observations (Egger & Aschenbach 1995): soft X-rays are absorbed by nearby neutral shell
- Possibly* result of interaction between LB and its neighbouring SB Loop I (Breitschwerdt+ 2000)
- Applied previous methodology on Loop I clusters Tr 10 and the Vel OB2 association to pin down generating SNe (19)

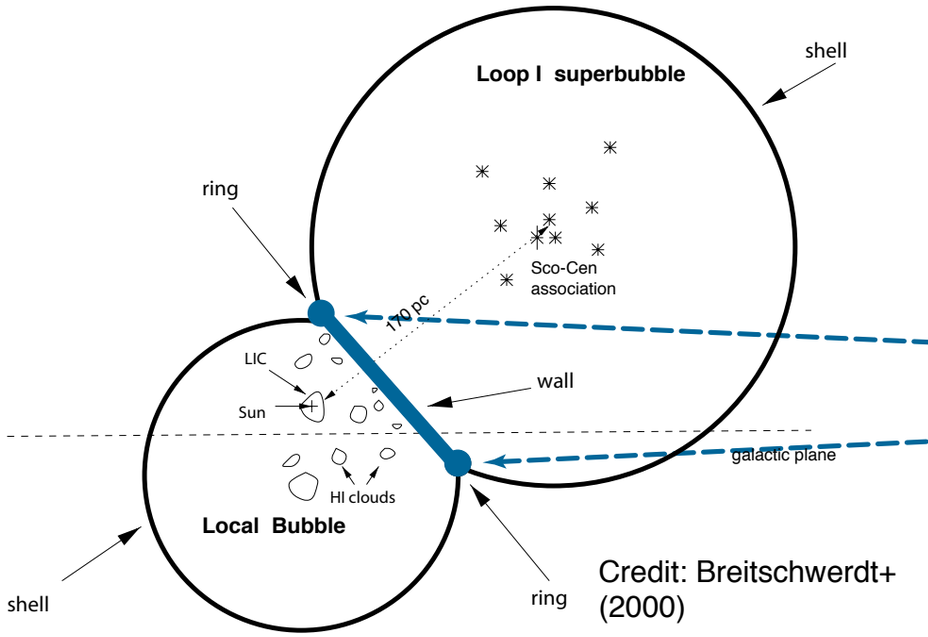

Credit: Breitschwerdt+ (2000)

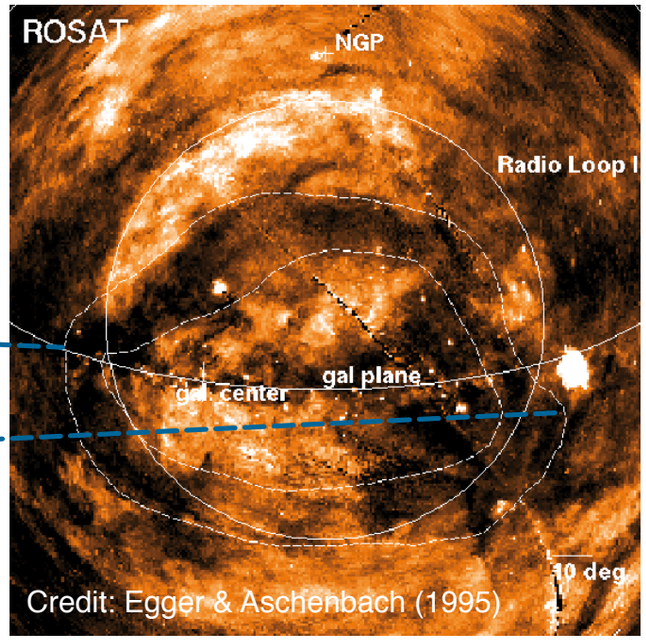

Credit: Egger & Aschenbach (1995)

* See special issue of journal *Galaxies:* "Searching for Connections among the Fermi Bubbles, the Galactic Center GeV Excess, and Loop I” (2018)

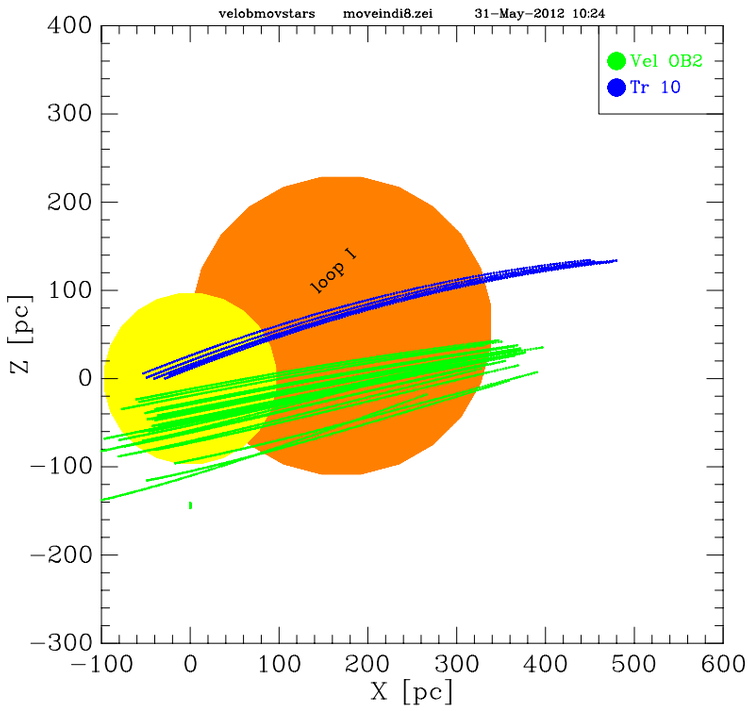

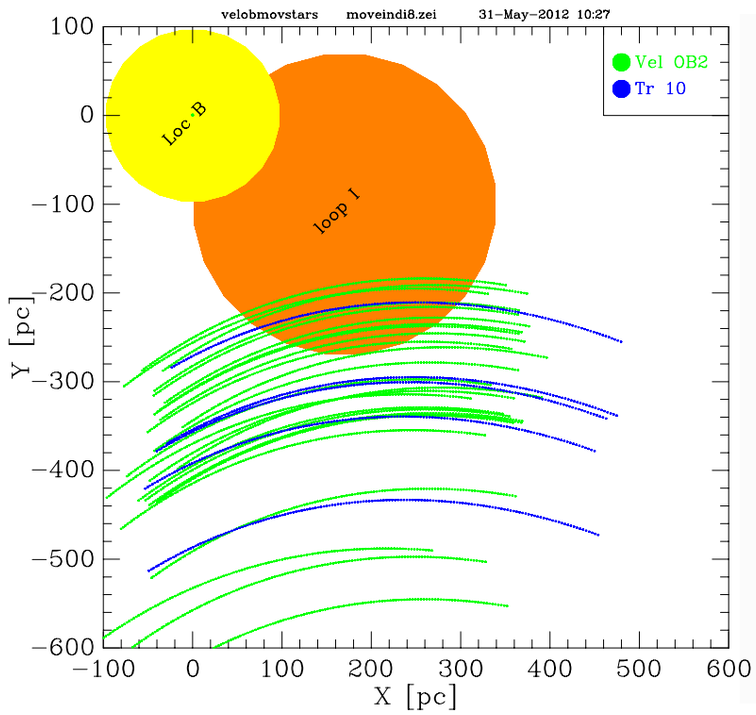

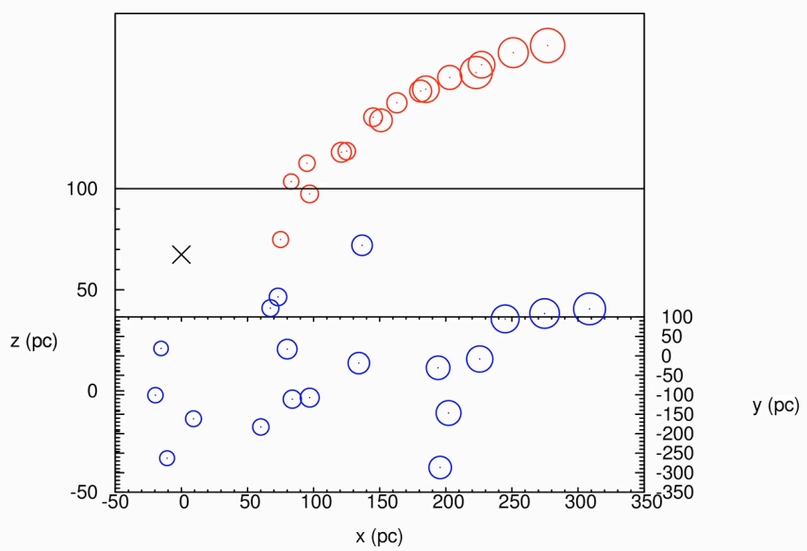

Calculating the amount of SN-released ^{60}Fe that arrives on Earth

1. Max. grid refinement around Sun → accurate ^{60}Fe flux in every time step
2. Fluxes are given at cell centres → average over eight grid cells
3. Compute time-integrated flux ('fluence'):

$$F = \frac{(\rho|\mathbf{u}|Z)_{\mathrm{VA}}}{\mathcal{A} m_{\mathrm{u}}} \Delta t$$

4. Surface density of atoms deposited on Earth at time t before present:

$$\Sigma(t) = \frac{fU}{4} F \exp\left(-t/t_{1/2}\right)$$

   - Assume isotropic fall-out (cf. Fry+ 2016)
   - **^{60}Fe survival fraction**, fU, only poorly known; dust factor $f \simeq 0.01$ (Fry+ 2015); uptake factor $U \simeq 0.5$–1 (Bishop & Egil 2011; Feige + 2012) → take either $fU = 0.006$ (cf. Knie+ 2004) or 0.005 (lower limit)

5. Obtain ^{60}Fe number density for each crust layer by summing Σ(t) over time intervals divided by thickness of layer
6. Relate n_{60Fe} to the density of stable iron (i.e. ^{60}Fe/Fe), given by

$$n_{\mathrm{Fe}} = \frac{x_{\mathrm{Fe}} \rho_{\mathrm{crust}} N_{\mathrm{A}}}{\mathcal{A}_{\mathrm{Fe}}} = 2.47 \times 10^{21}\ \mathrm{cm}^{-3}$$

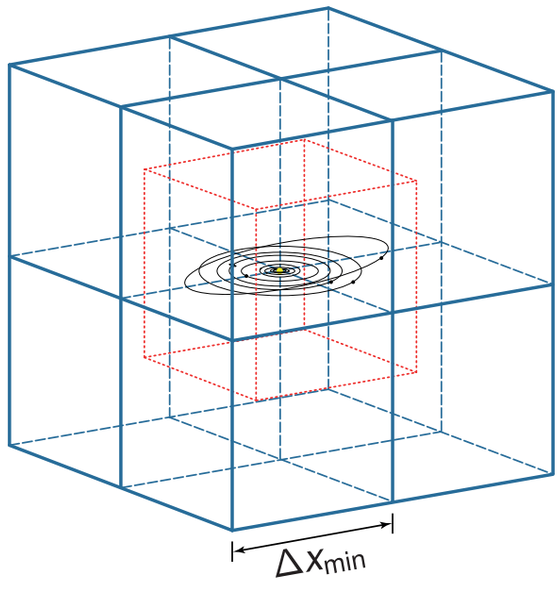

Chemical mixing simulations with homogeneous background medium

Evolution of the gas column density distribution (cuts through $z = 0$ and $y = 0$)

Model A (~ WIM)

$n = 0.1\ cm^{-3}$

$T = 10^4\ K$

$Z/Z_\odot = 1$

$\Delta x = 0.7\ pc$

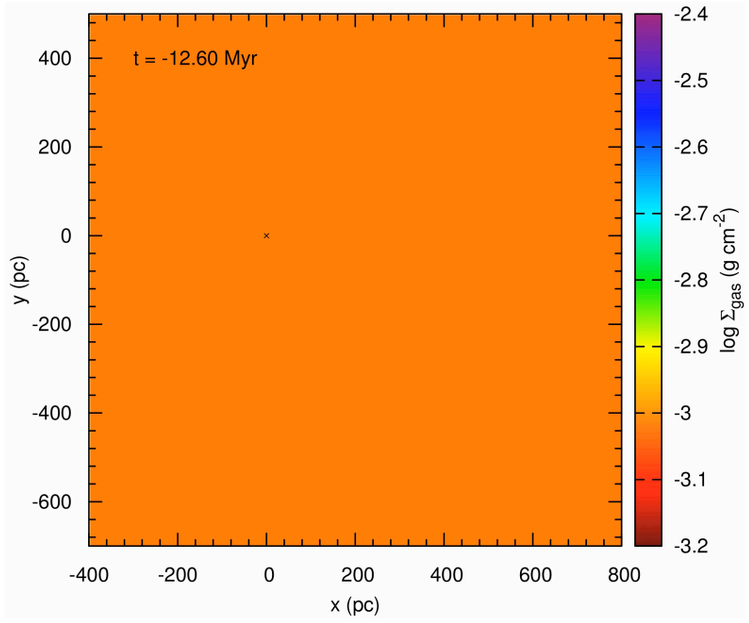

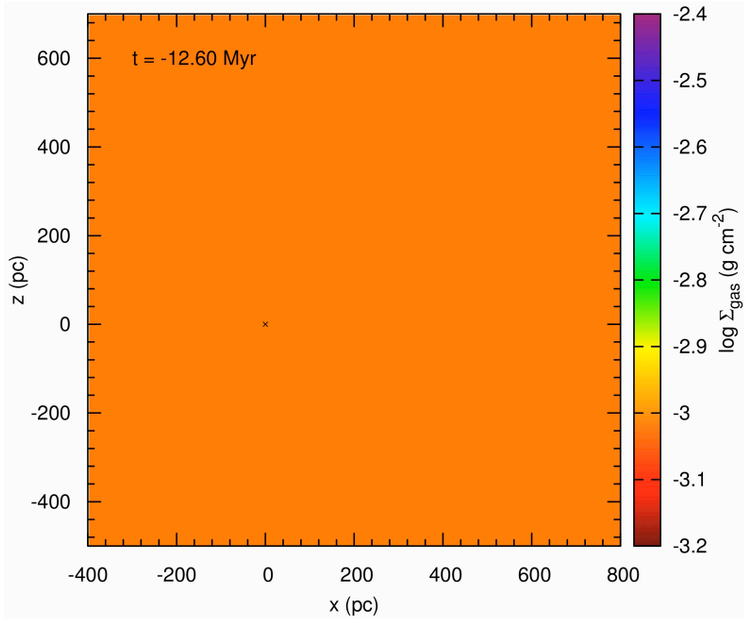

Model B (~ WNM)

$n = 0.3\ cm^{-3}$

$T = 6800\ K$

$Z/Z_\odot = 1$

$\Delta x = 0.7\ pc$

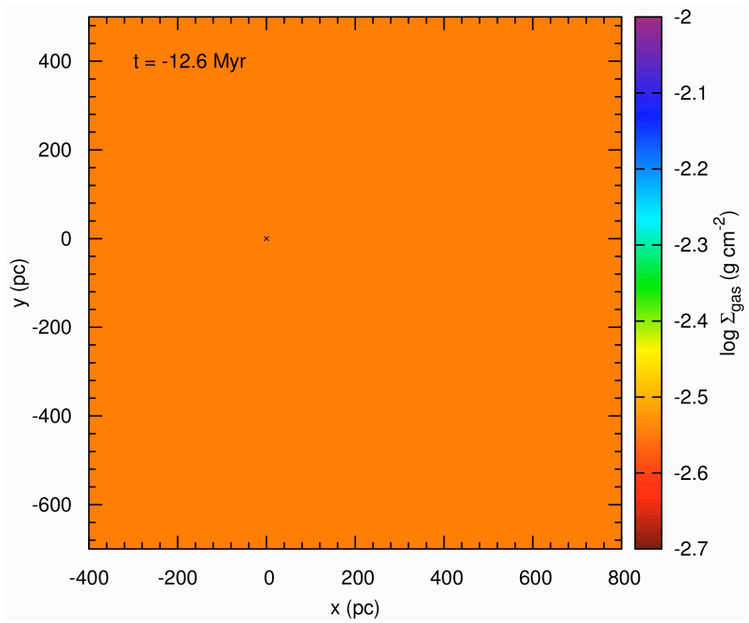

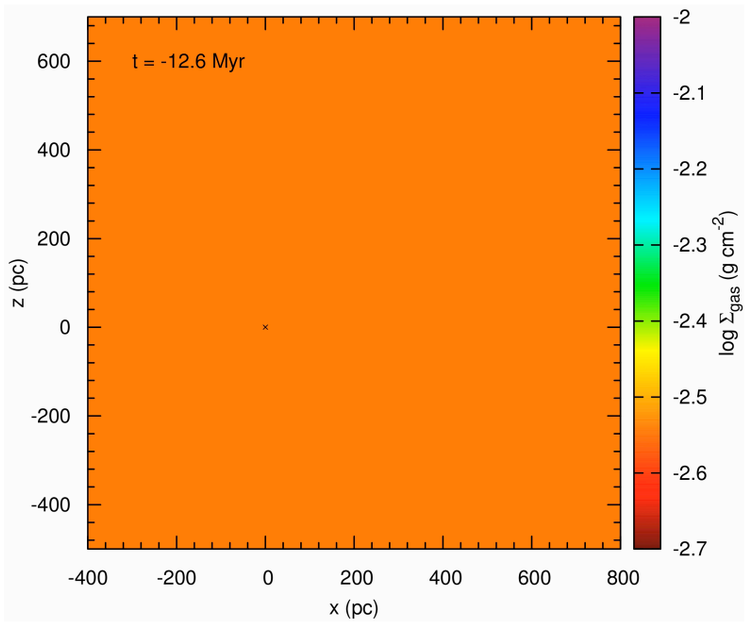

Chemical mixing simulations with homogeneous background medium

Volume rendering of the present-day density distribution

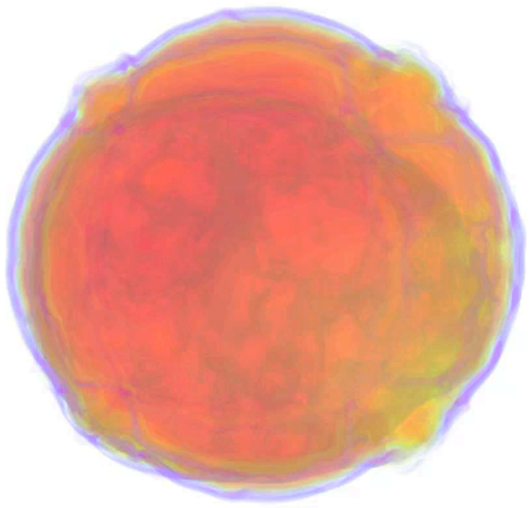

Model A

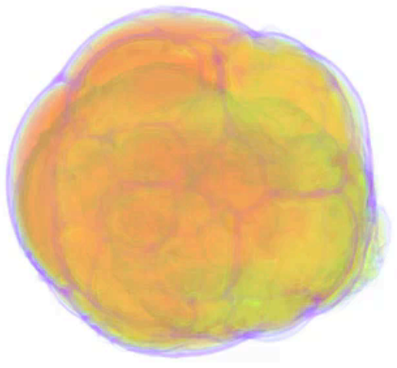

Model B

- LB and Loop I form almost coevally
- **At first:** independent evolution, formation of cold, dense clumps due to instabilities
- **Later on:** shells collide after 3.0 (model A) and 4.6 Myr (model B) → RT unstable interaction layer
- Shells break-up after 6.5 Myr (model A) or never (model B)
- 'Present' LB extension: (x,y,z) = (800,600,760) pc in model A; (580,480,540) pc in model B
- Hydrogen density and temperature in 'present' LB cavity: $10^{-4.2}$–$10^{-3.9}$ cm^{-3}, $10^{6.9}$–$10^{7.1}$ K in model A; $10^{-4.2}$–10^{-3} cm^{-3}, $10^{5.8}$–10^{7} K in model B
- Agreement between computed and observed extension of bubbles poor → ambient medium not known
- Exact extensions not crucial for ^{60}Fe transport modelling as long as the solar system resides within the LB; exception: supershell arrival

Chemical mixing simulations with homogeneous background medium

Evolution of the ^{60}Fe mass density distribution (cuts through $z = 0$ and $y = 0$)

Model A (~ WIM)

$n = 0.1$ cm^{-3}

$T = 10^4$ K

$Z/Z_\odot = 1$

$\Delta x = 0.7$ pc

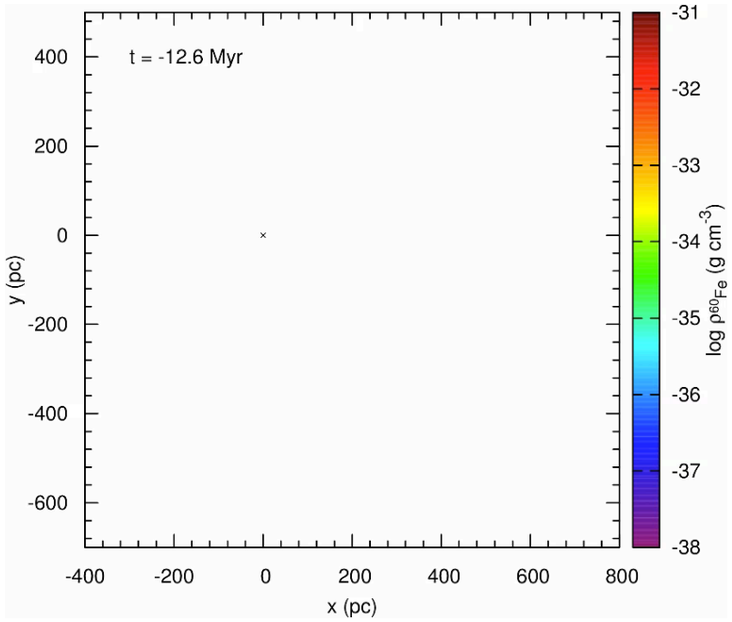

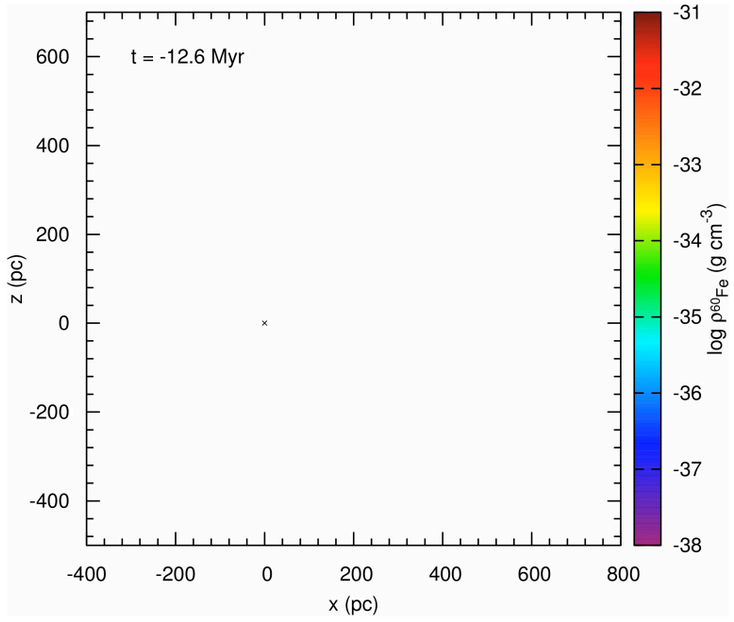

Model B (~ WNM)

$n = 0.3$ cm^{-3}

$T = 6800$ K

$Z/Z_\odot = 1$

$\Delta x = 0.7$ pc

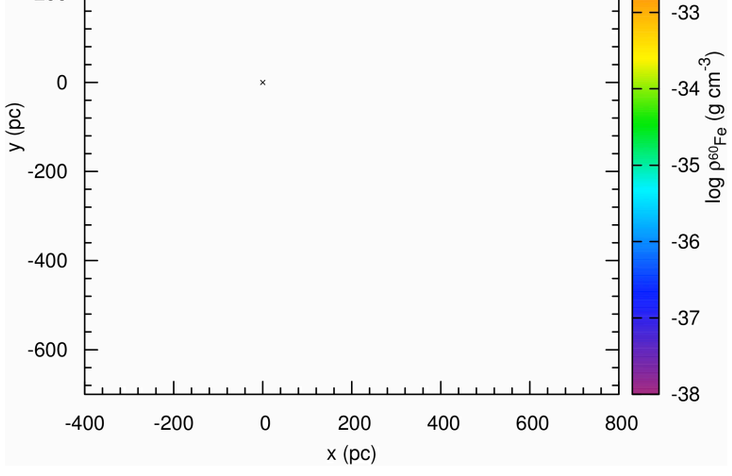

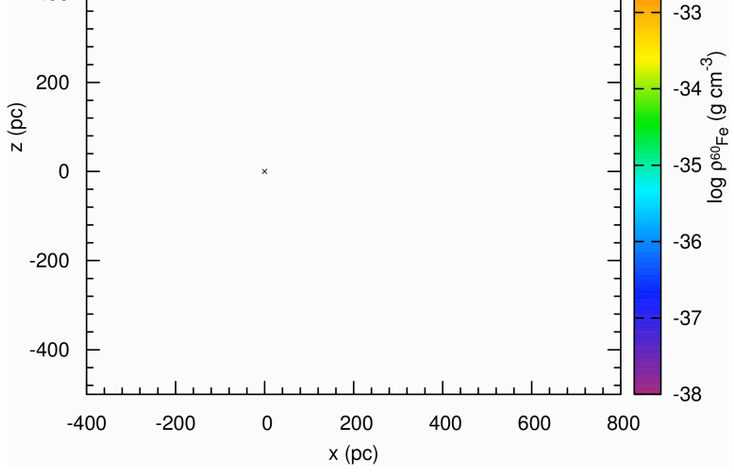

- Inhomogeneities arising from recent SNe are smoothed out over time
- Injection of turbulence by SNRs running into supershell → generating asymmetric reflected shocks

- Time scale of mixing: $\tau_m \lesssim \ell/a$ = (100 pc)/(100 km s^{-1}) = 1 Myr
- ^{60}Fe fairly homogenized since last LB SN occurred about 1.5 Myr ago

Chemical mixing simulations with homogeneous background medium

Model A: Entropy maps and ^{60}Fe fluence variation

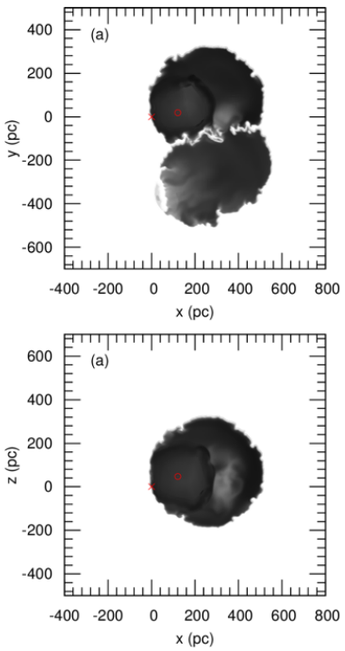

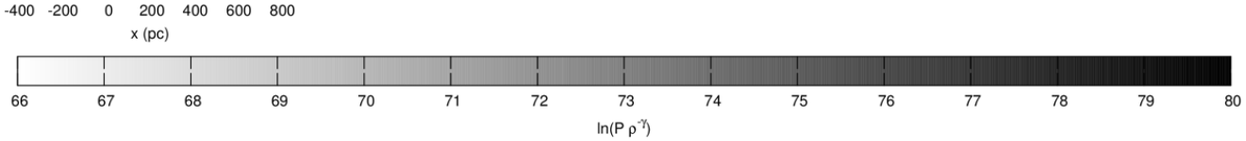

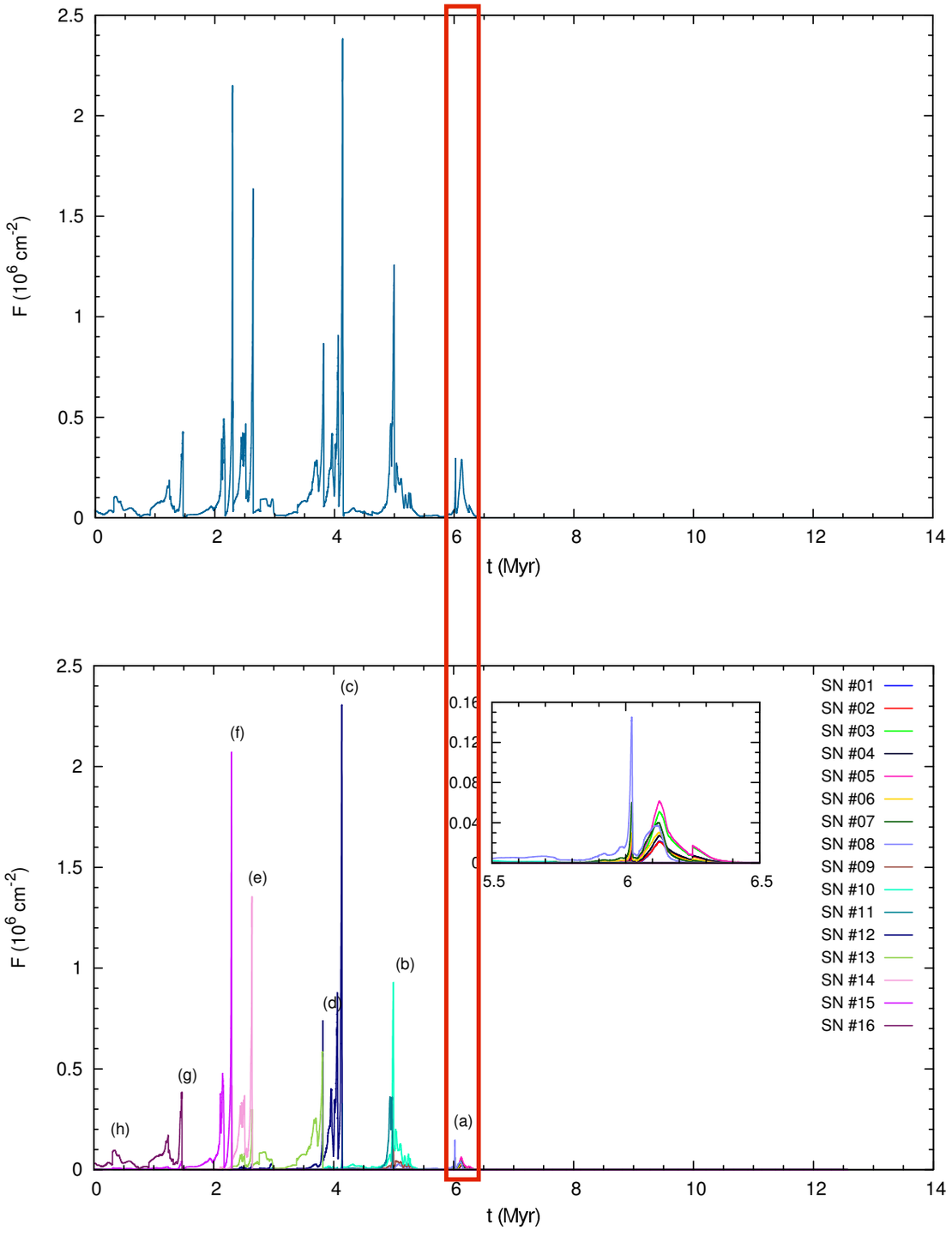

Chemical mixing simulations with homogeneous background medium

Model A: Entropy maps and ^{60}Fe fluence variation

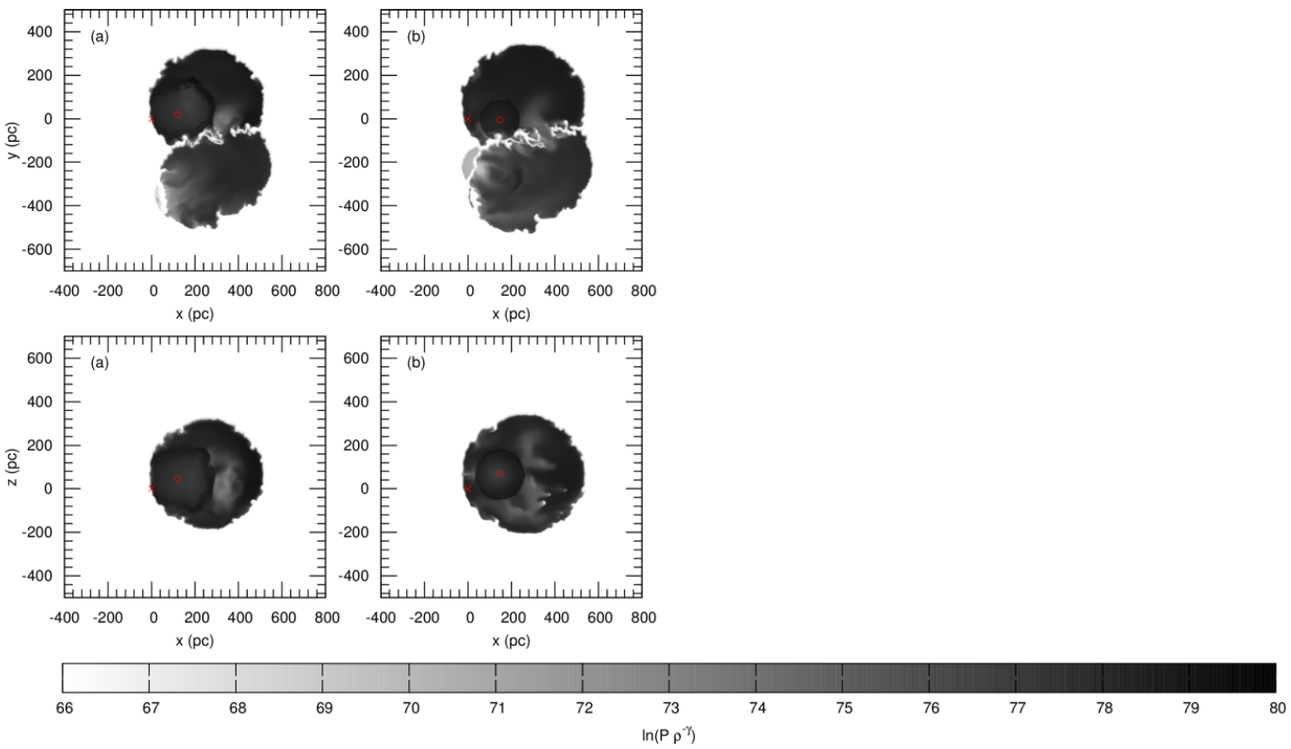

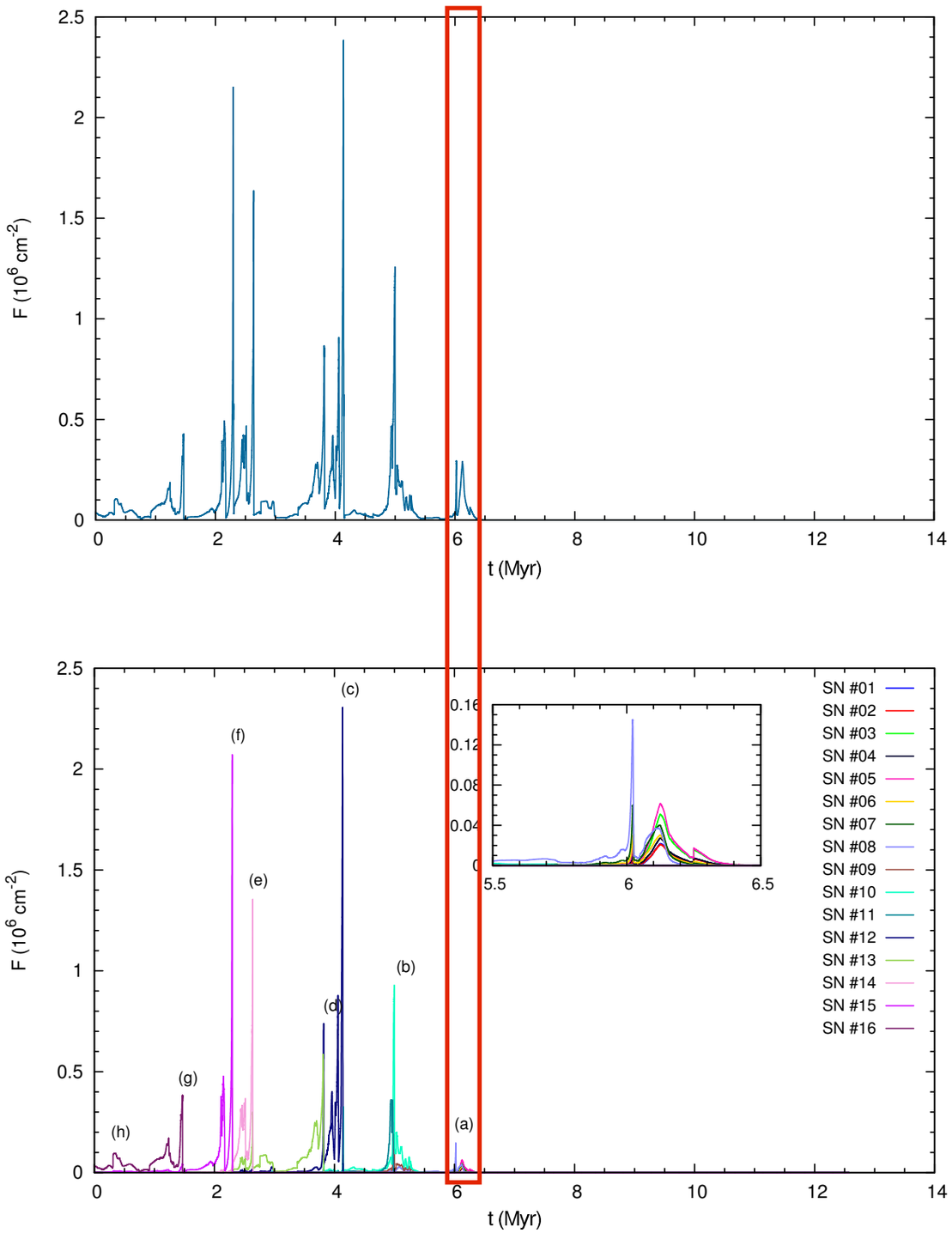

Chemical mixing simulations with homogeneous background medium

Model A: Entropy maps and ^{60}Fe fluence variation

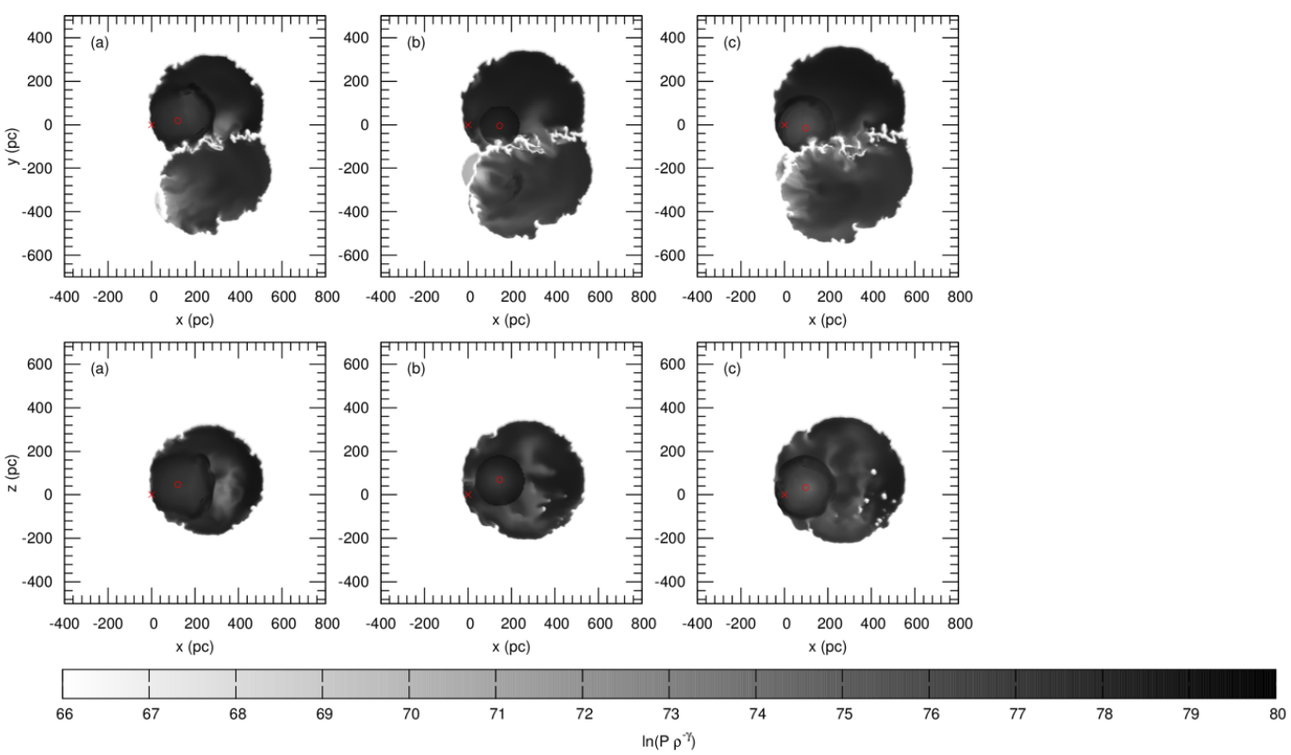

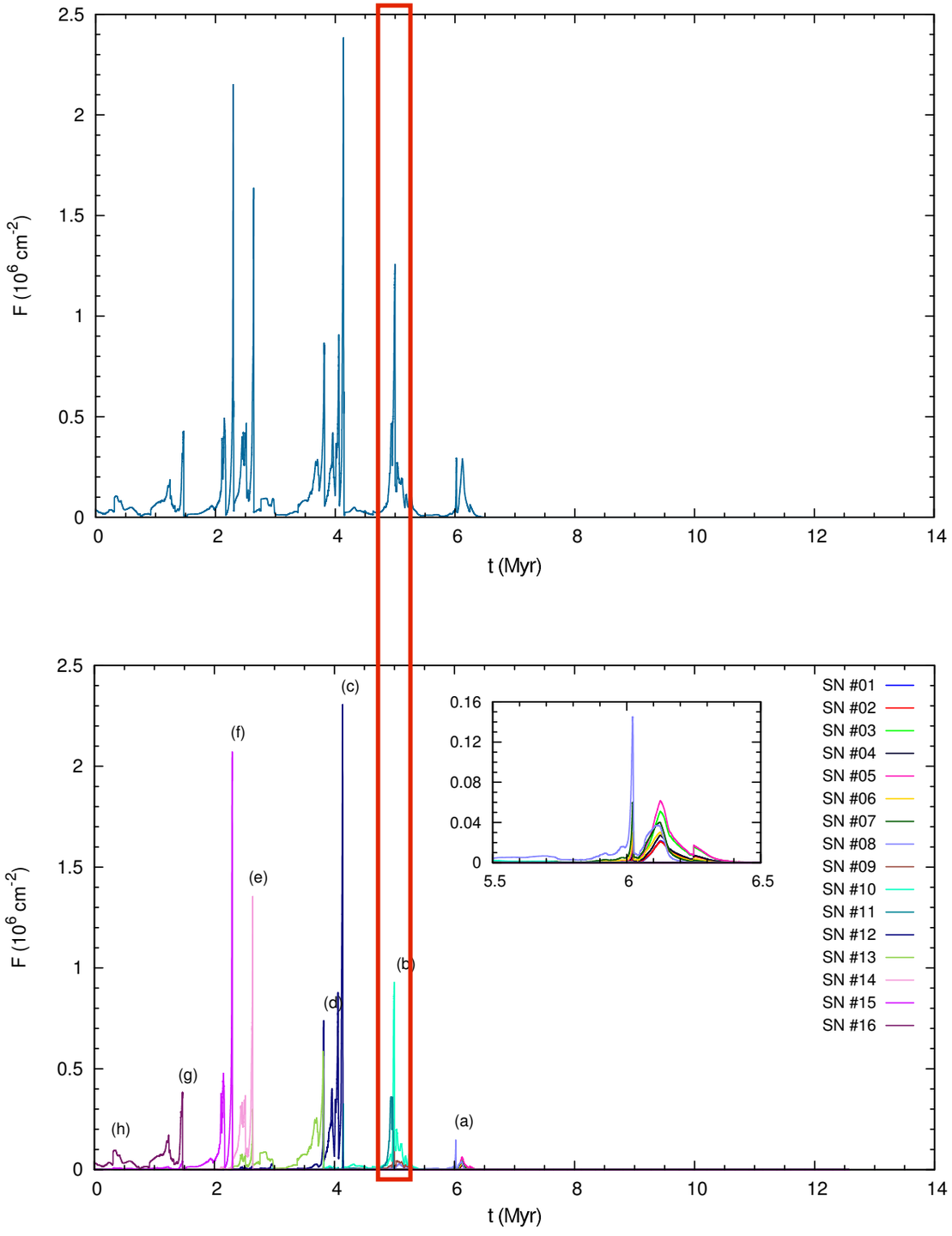

Chemical mixing simulations with homogeneous background medium

Model A: Entropy maps and ^{60}Fe fluence variation

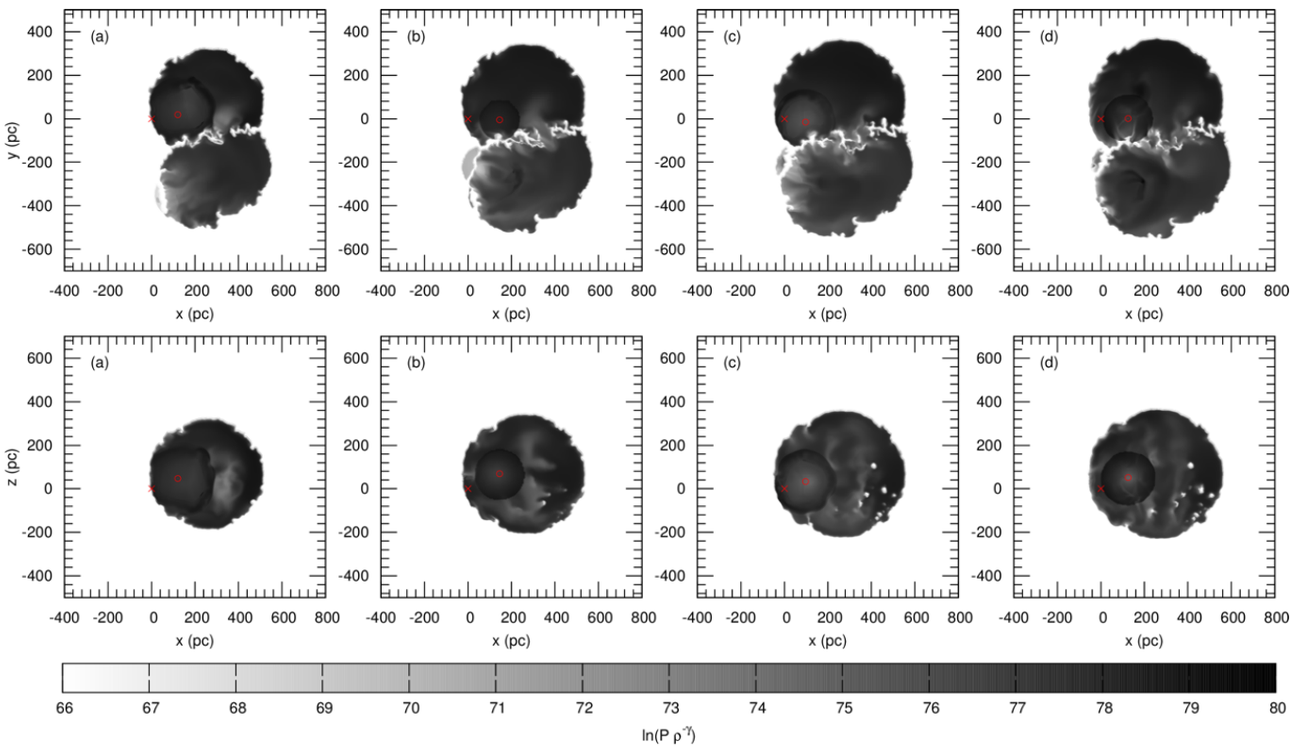

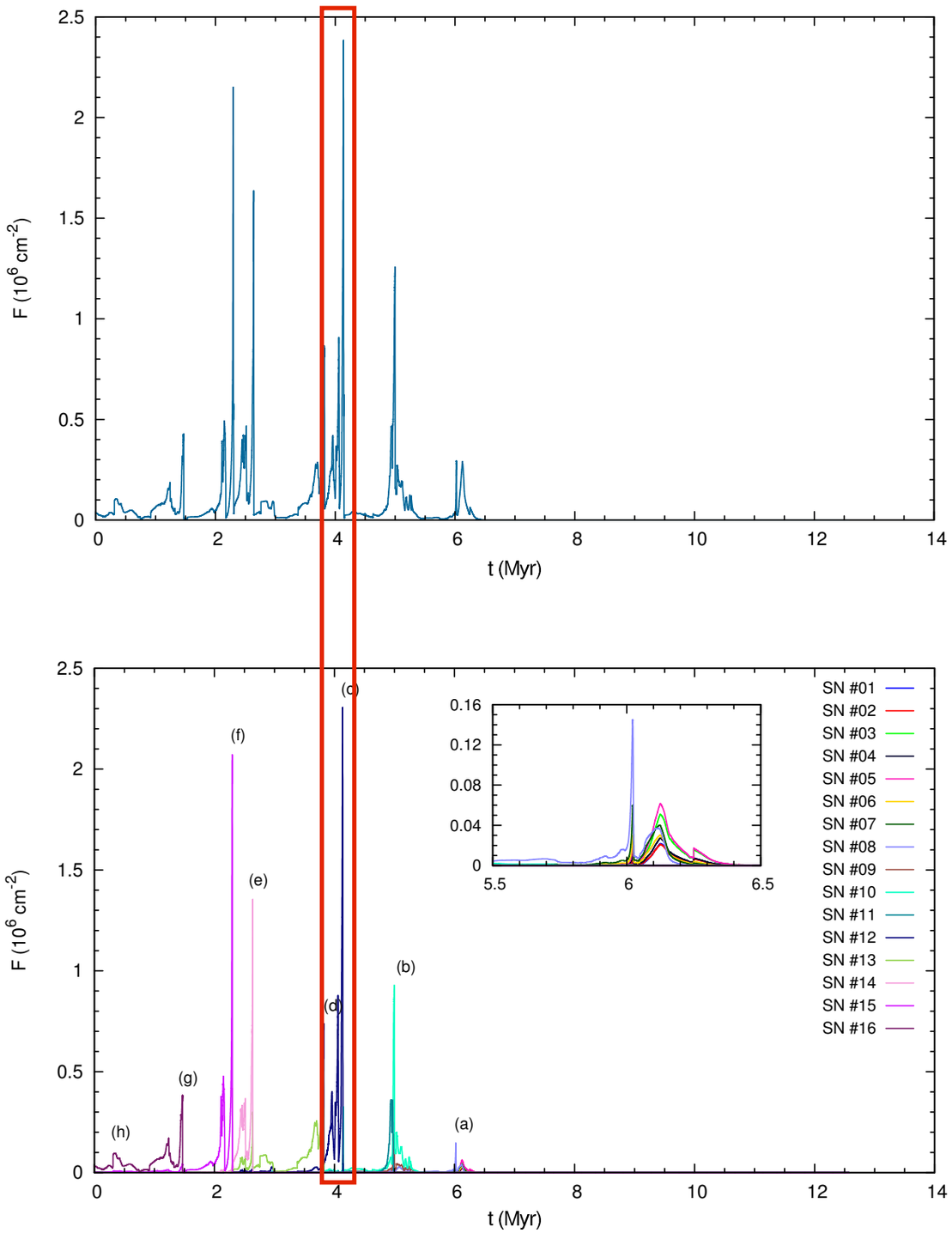

Chemical mixing simulations with homogeneous background medium

Model A: Entropy maps and ^{60}Fe fluence variation

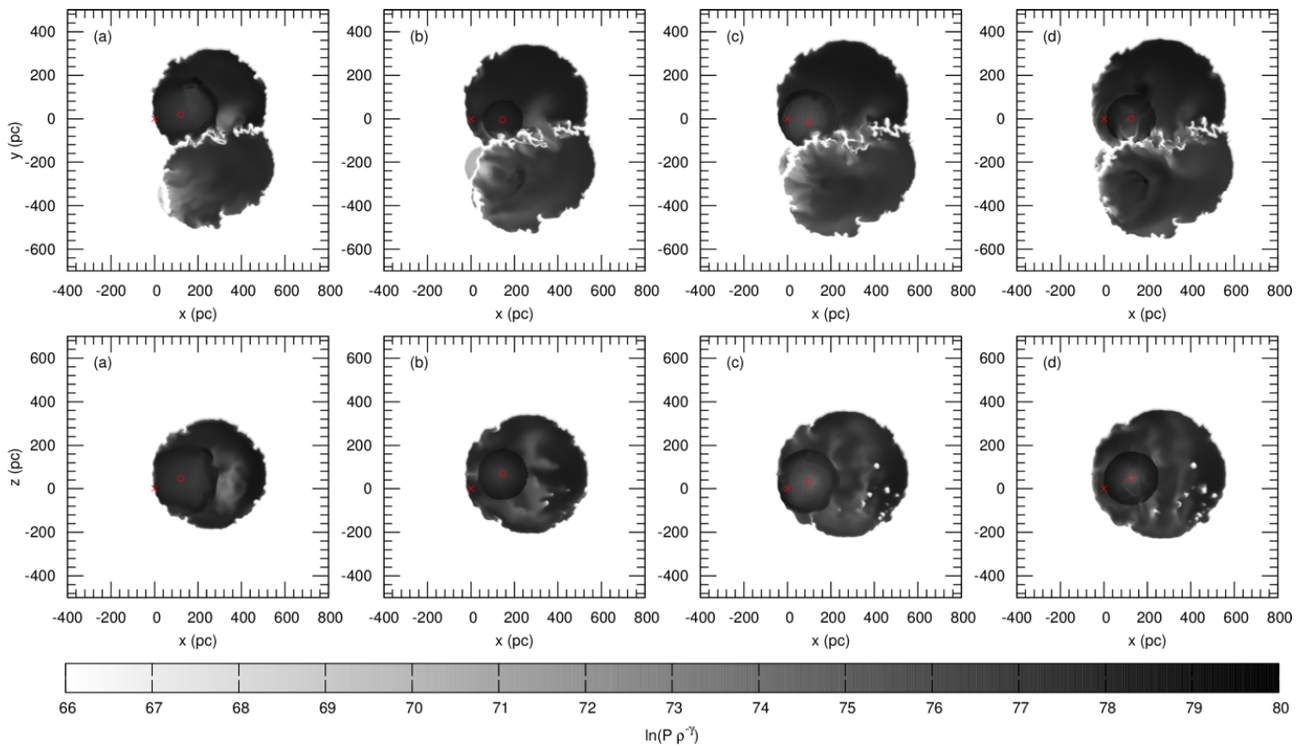

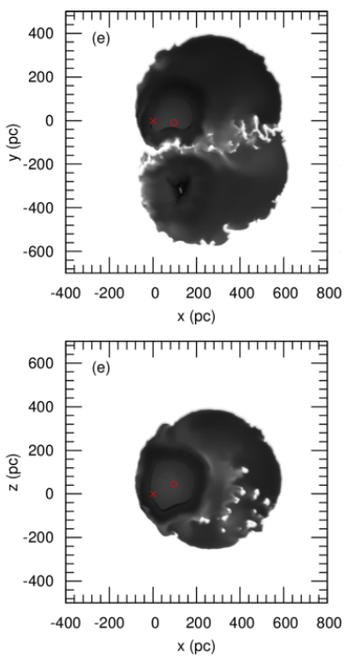

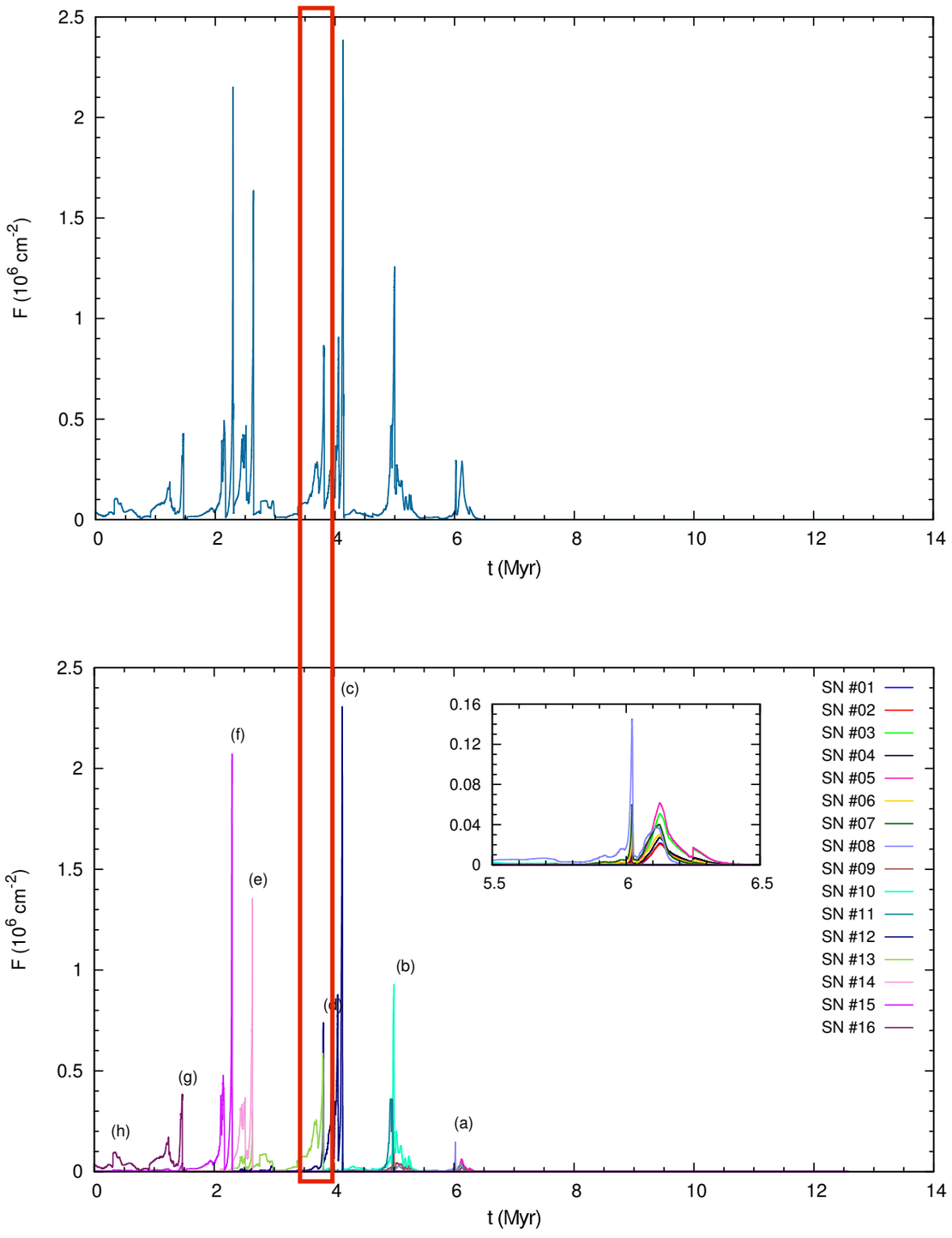

Chemical mixing simulations with homogeneous background medium

Model A: Entropy maps and ^{60}Fe fluence variation

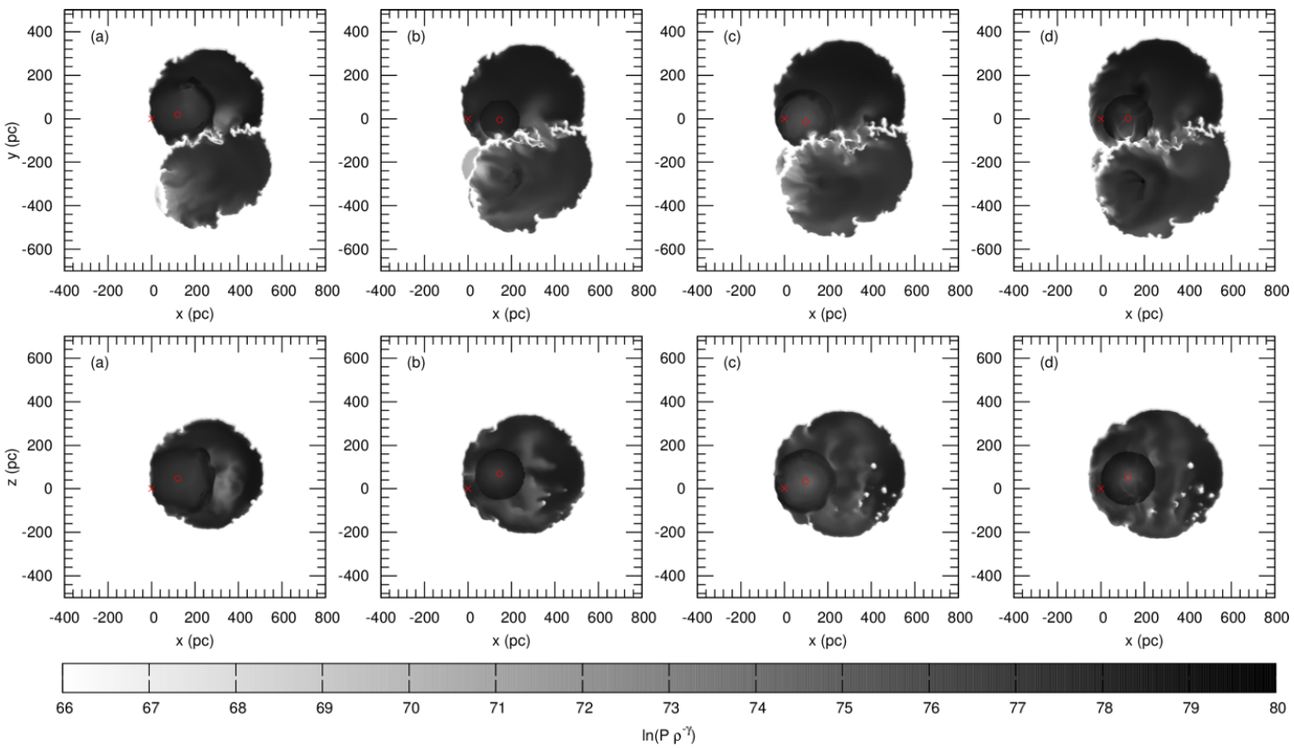

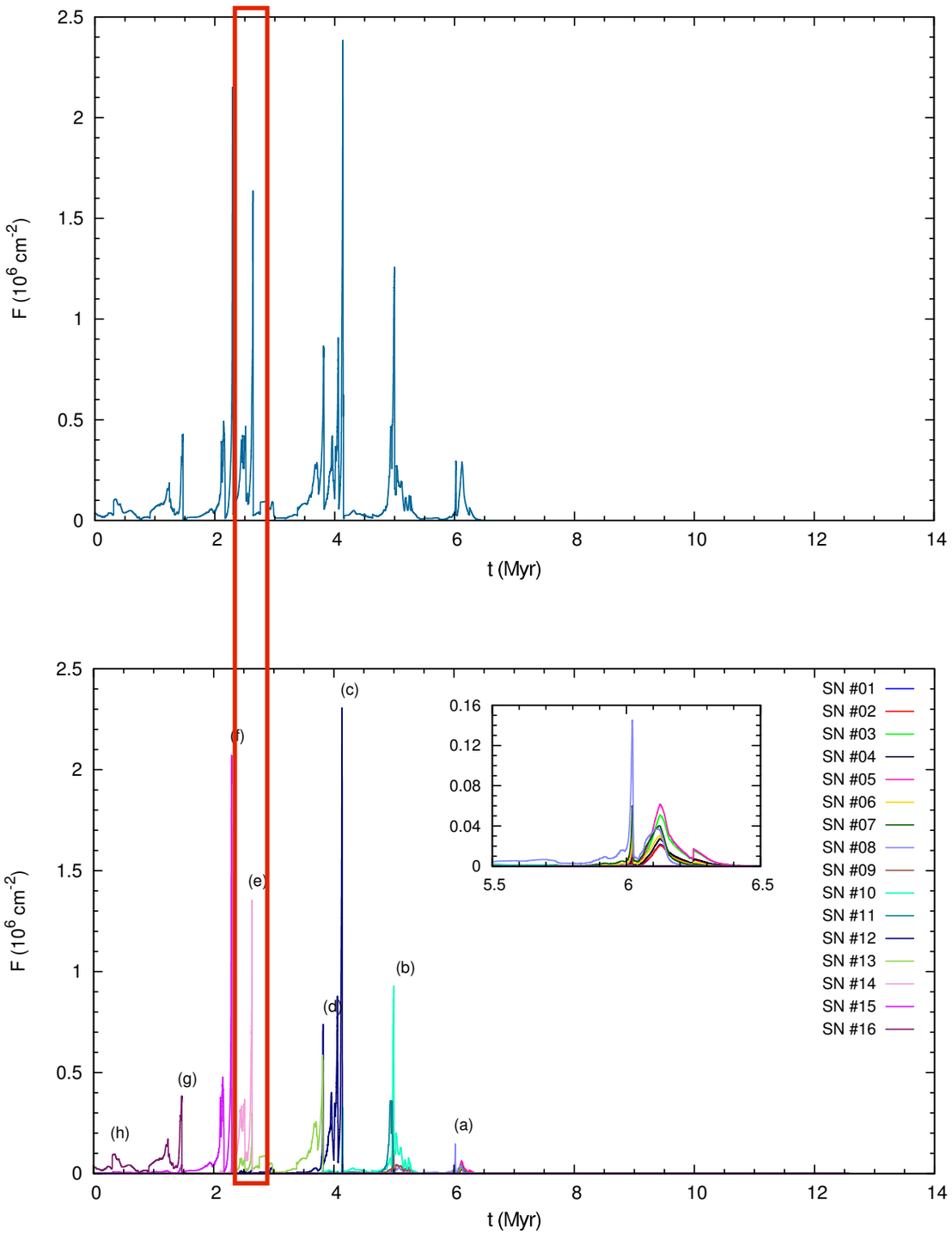

Chemical mixing simulations with homogeneous background medium

Model A: Entropy maps and ^{60}Fe fluence variation

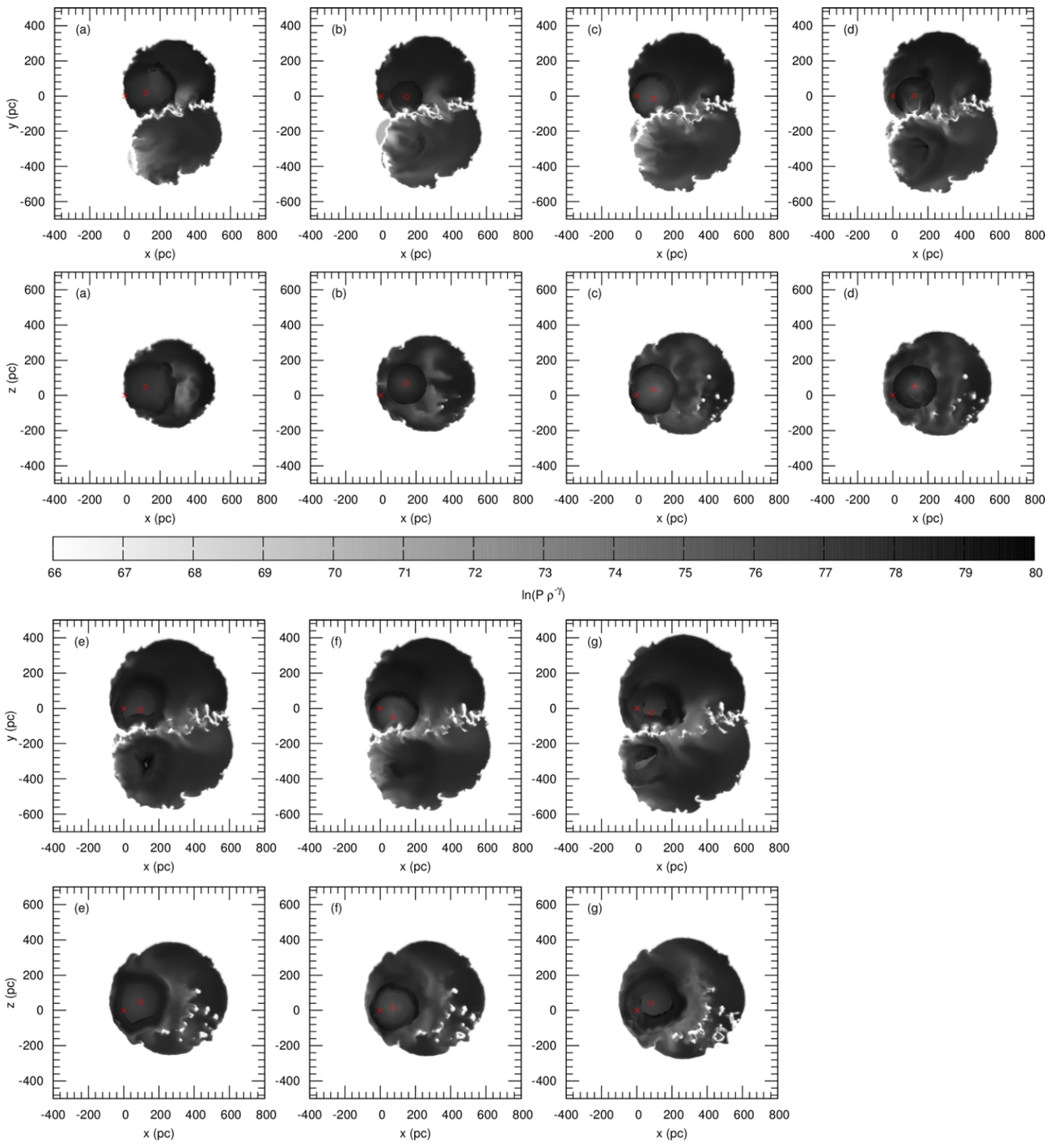

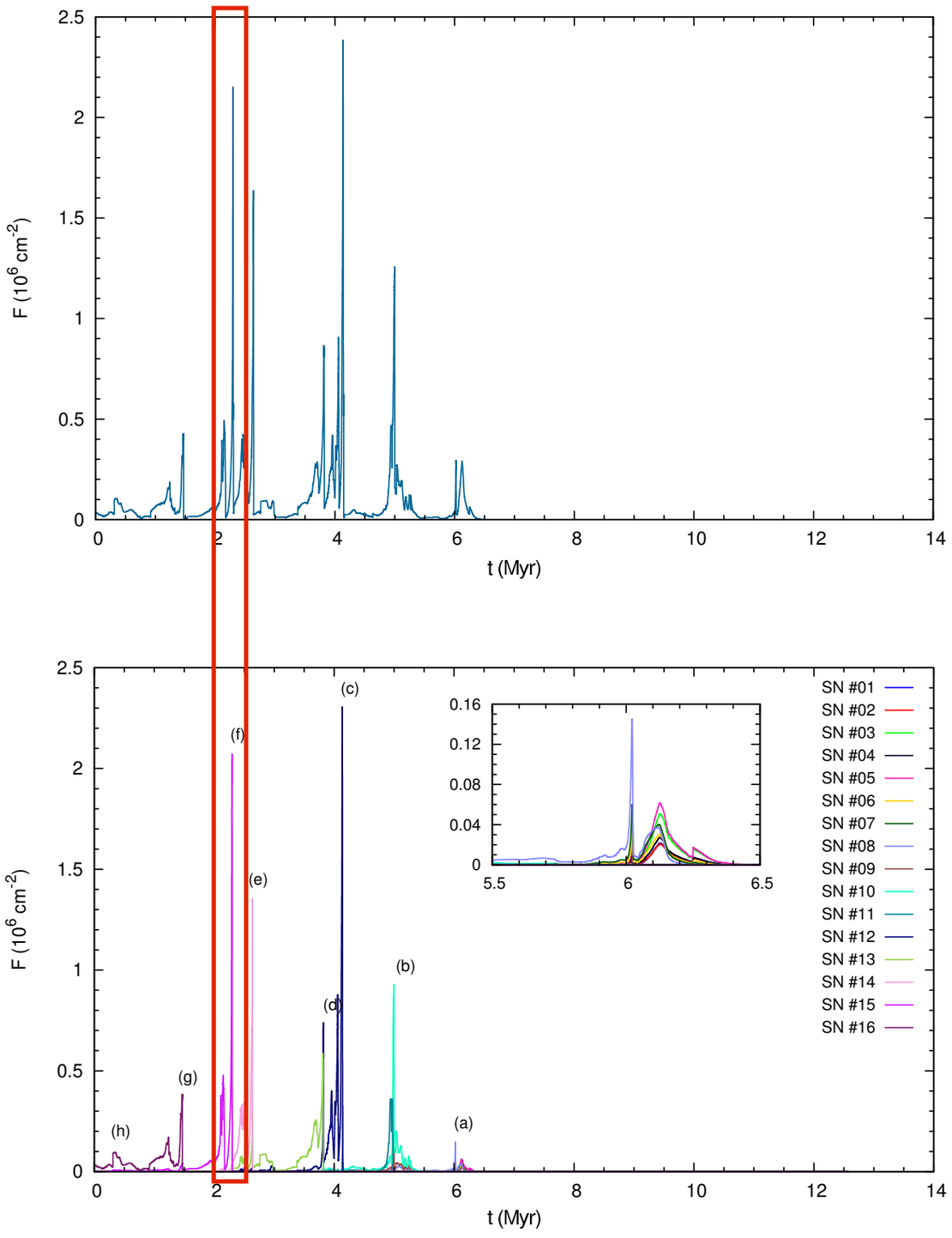

Chemical mixing simulations with homogeneous background medium

Model A: Entropy maps and ^{60}Fe fluence variation

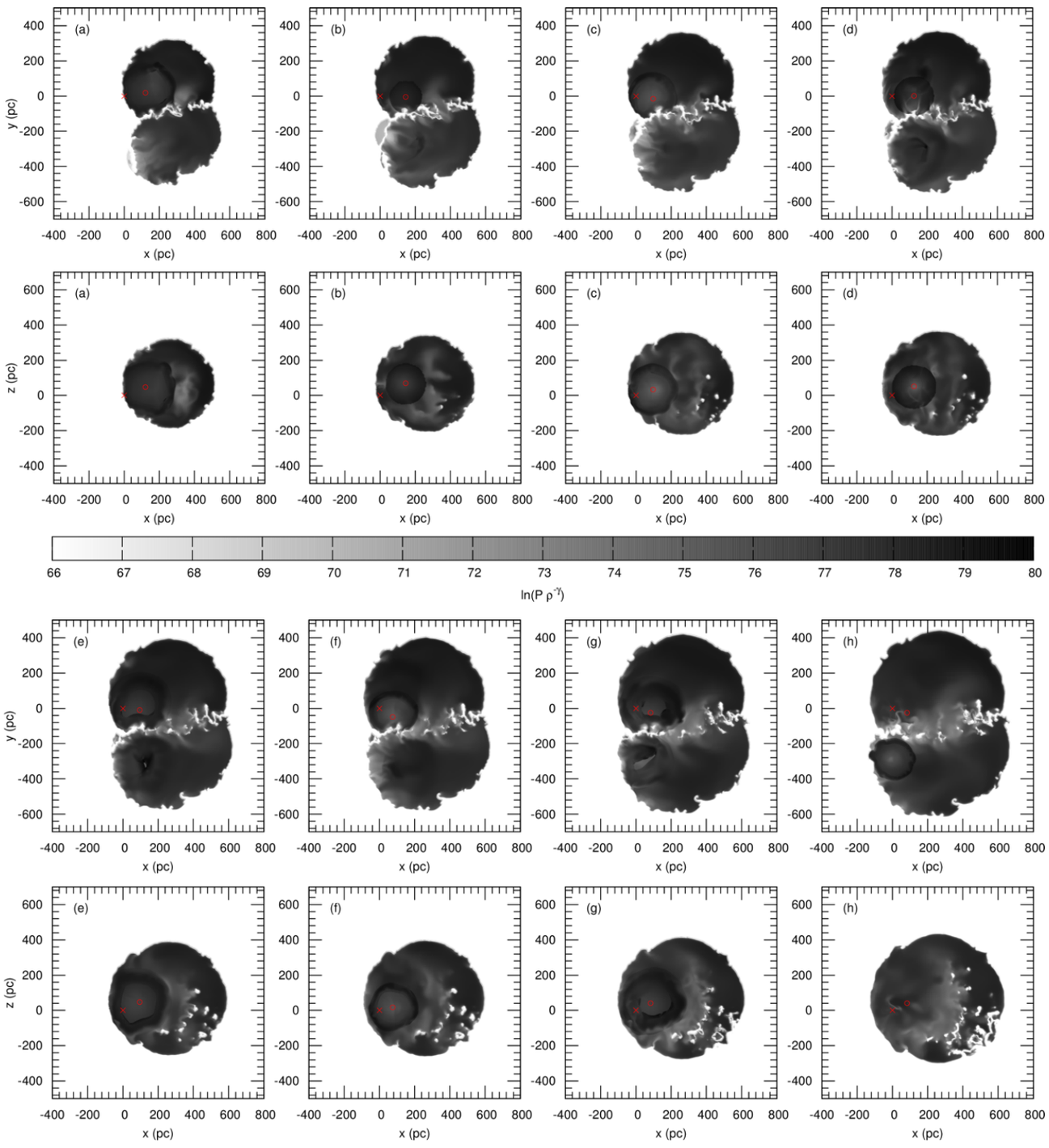

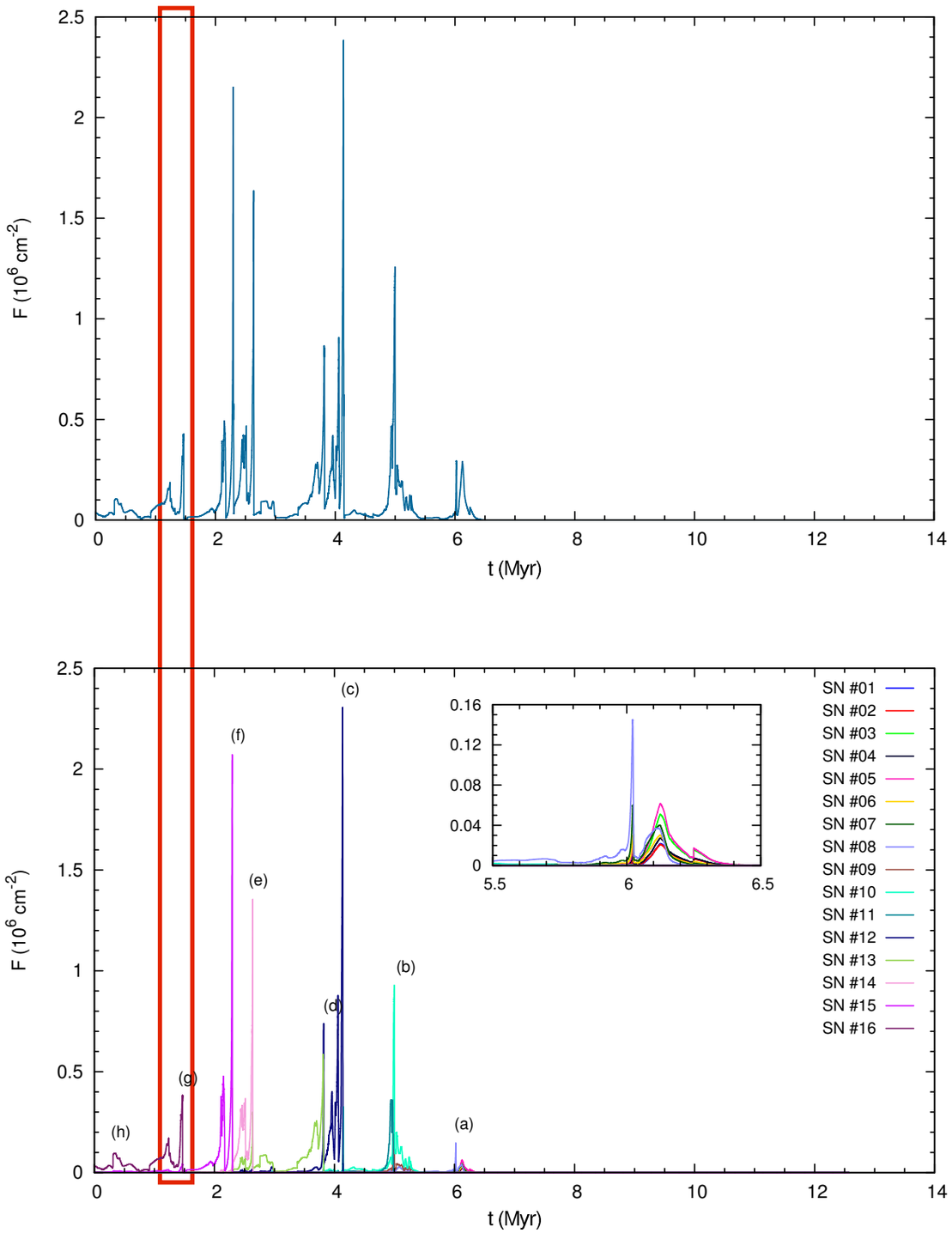

Chemical mixing simulations with homogeneous background medium

Model A: Entropy maps and modeled ^{60}Fe/Fe content in the FeMn crust

- Three different types of signals:
  1. High and sharp sawtooth waves → Sedov-Taylor-phase SNRs (exposure time: $\Delta t \simeq$ 70–130 kyr ~ shell thickness)
  2. Weaker, more extended signals trailing sawtooth waves → blast wave reflected from supershell (*SN 'echoes'*)
  3. Broad signal at the beginning of the profile ($\Delta t \gtrsim$ 300 kyr) → LB supershell arrival
- All pulses entrain fractions of previously released ^{60}Fe
- ^{60}Fe should arrive on Earth as **dust**:
  - 'Filtering' due to partial condensation, loss during SNR expansion, collision between SNR and solar wind bubble
  - Remaining $f \simeq 1\%$ with grain sizes $\lesssim 0.2\ \mu$m (Fry+ 2015) travel almost ballistically through solar system
  - Combined with recent uptake factor, $U = 0.5$–1 (Bishop & Egli 2011; Feige+ 2012) → lower limit of survival fraction: $fU \simeq 0.005$

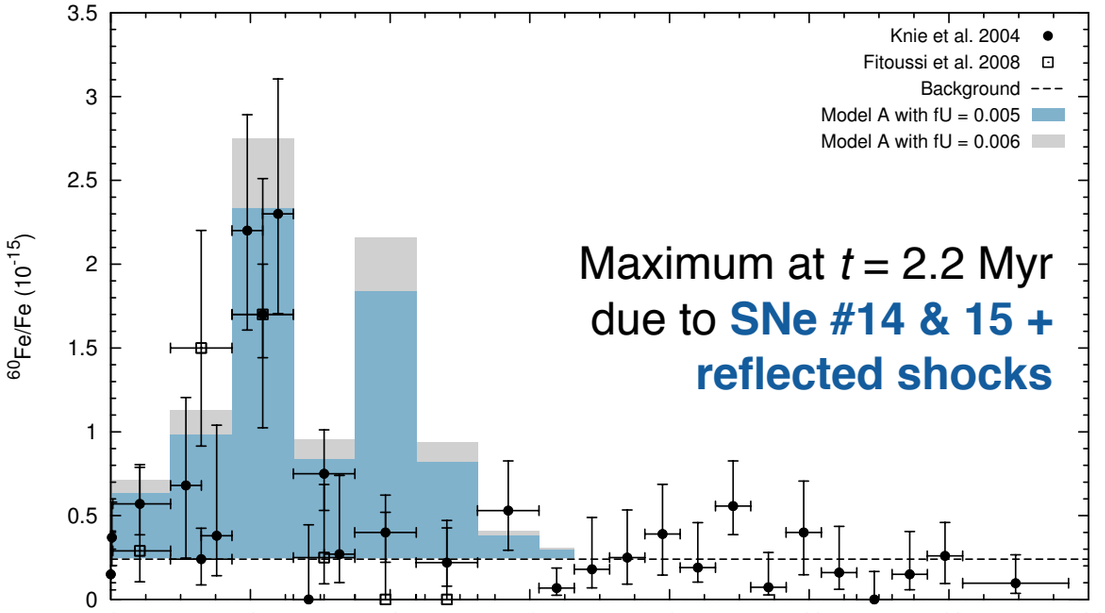

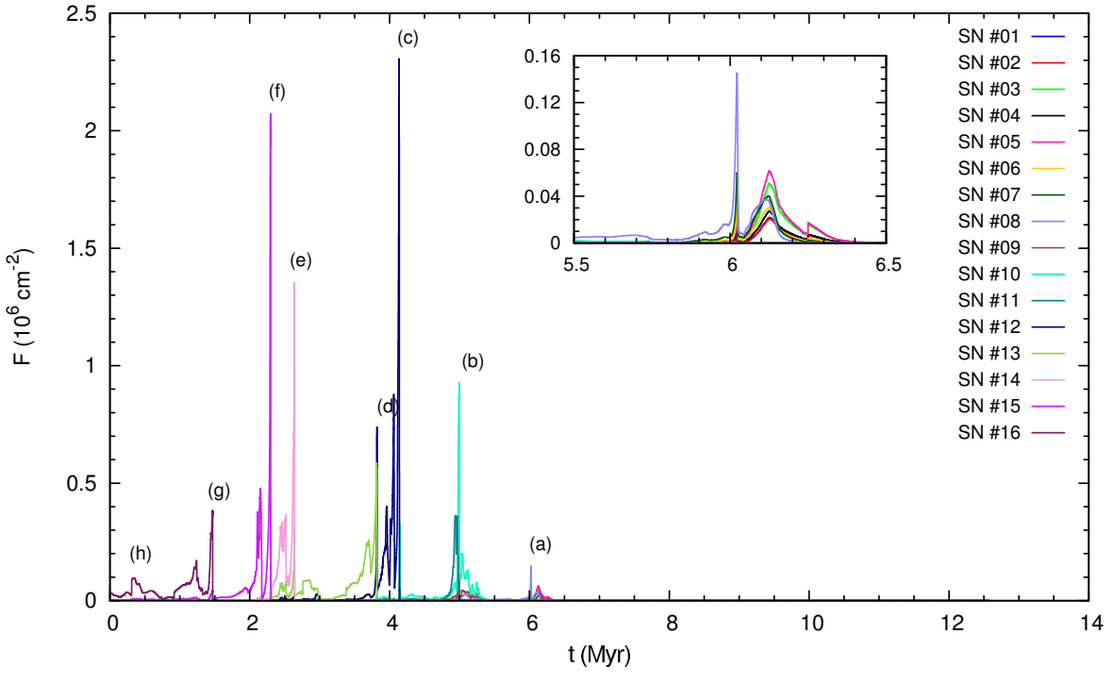

Chemical mixing simulations with homogeneous background medium

Model B: Entropy maps and 60Fe fluence variation

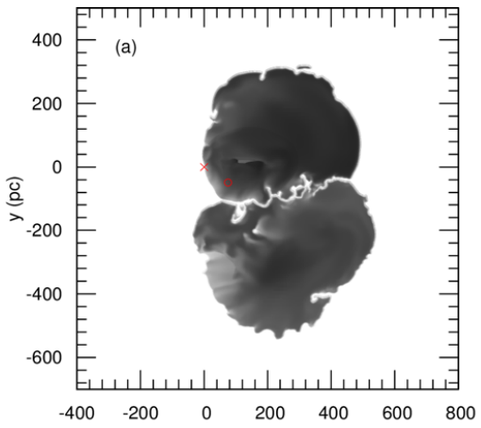

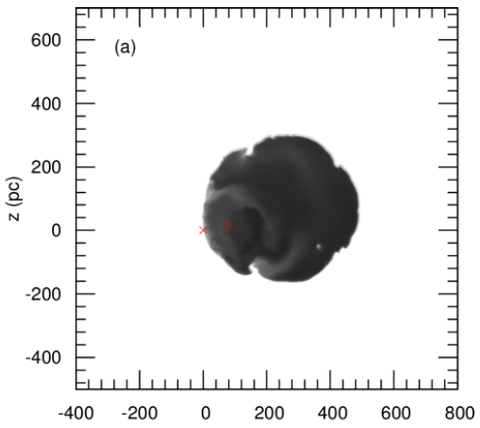

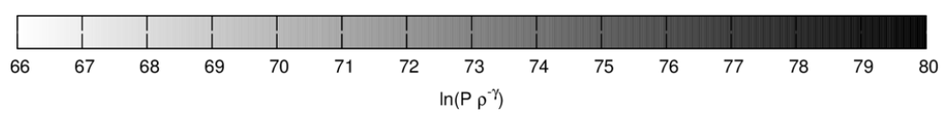

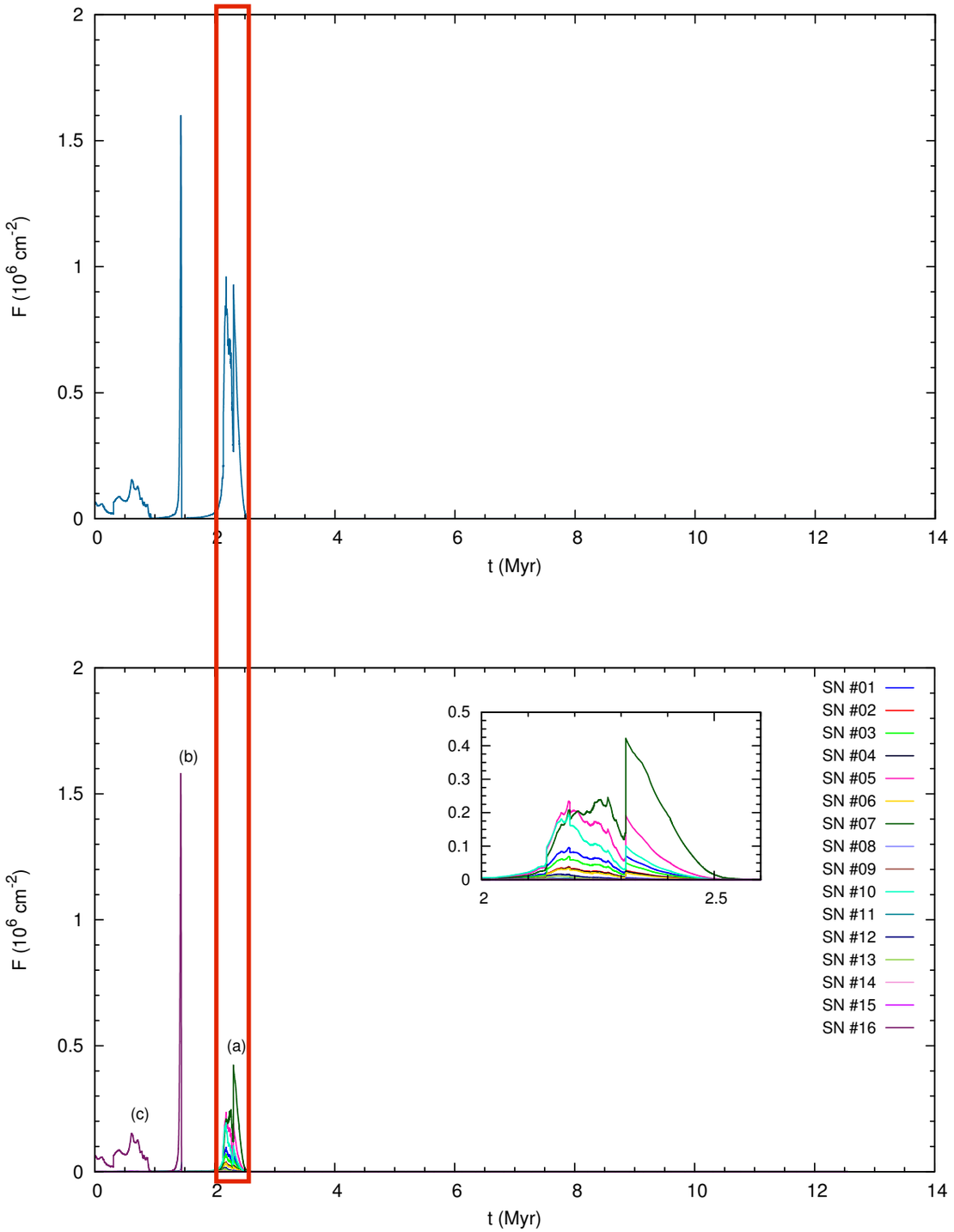

Chemical mixing simulations with homogeneous background medium

Model B: Entropy maps and 60Fe fluence variation

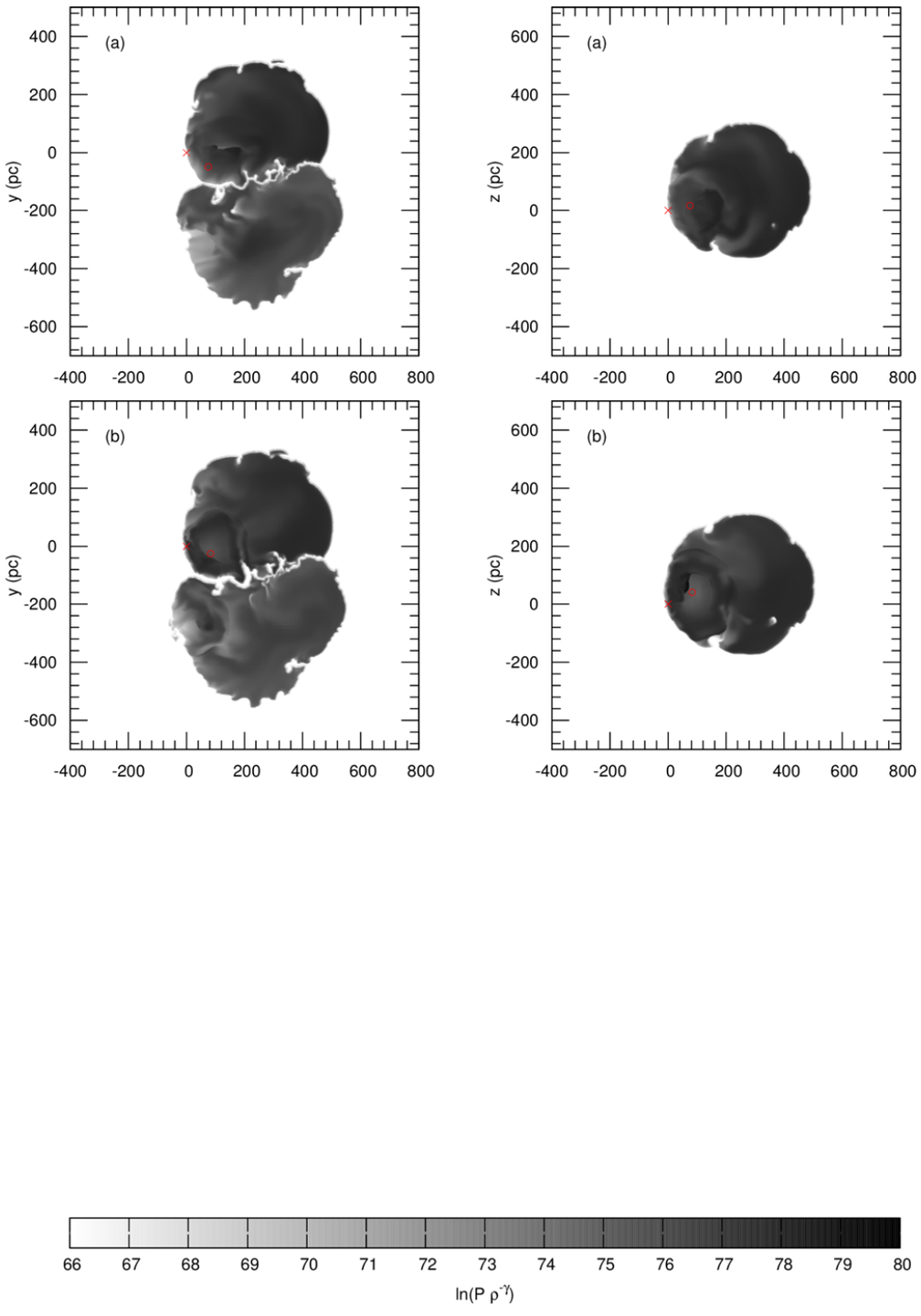

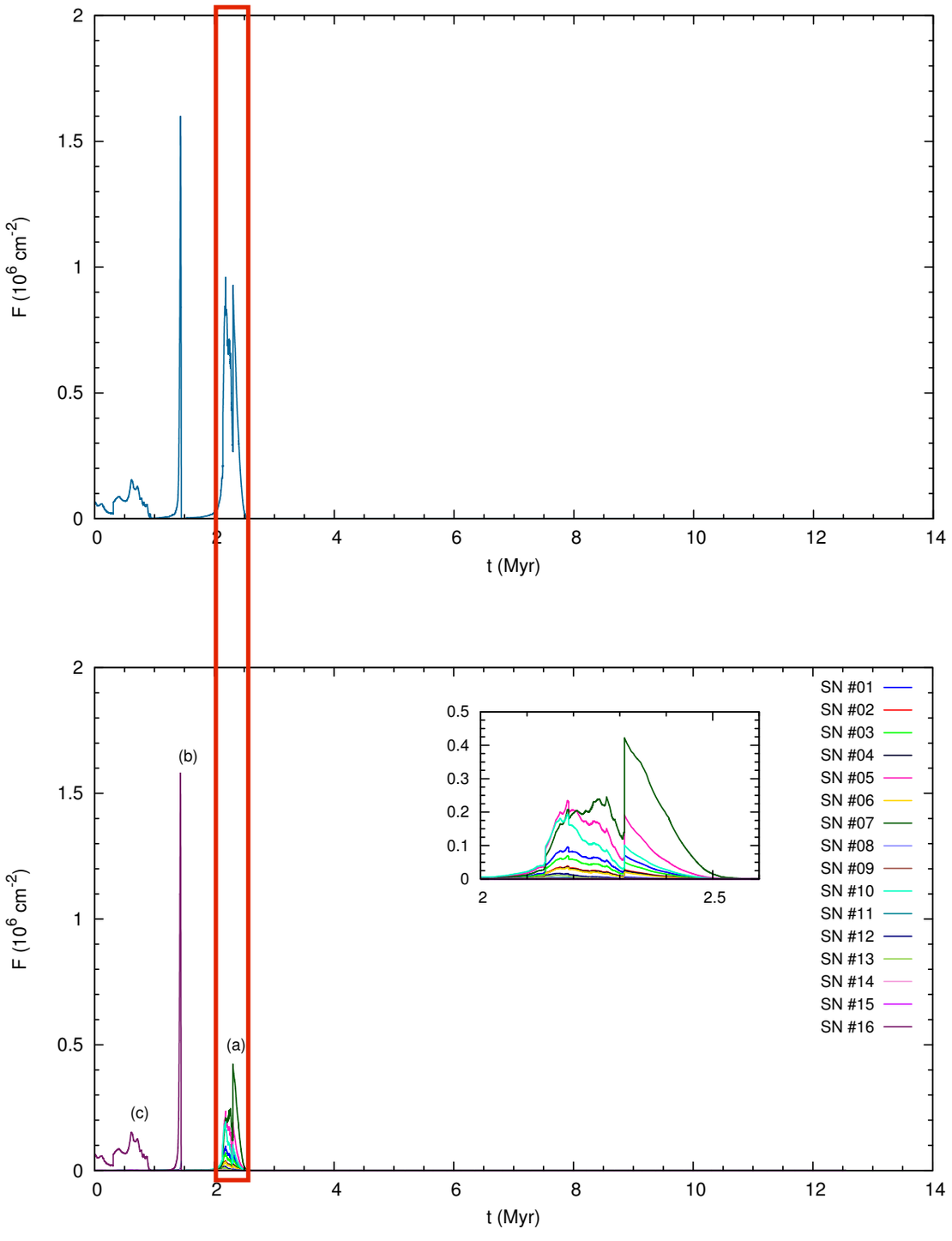

Chemical mixing simulations with homogeneous background medium

Model B: Entropy maps and 60Fe fluence variation

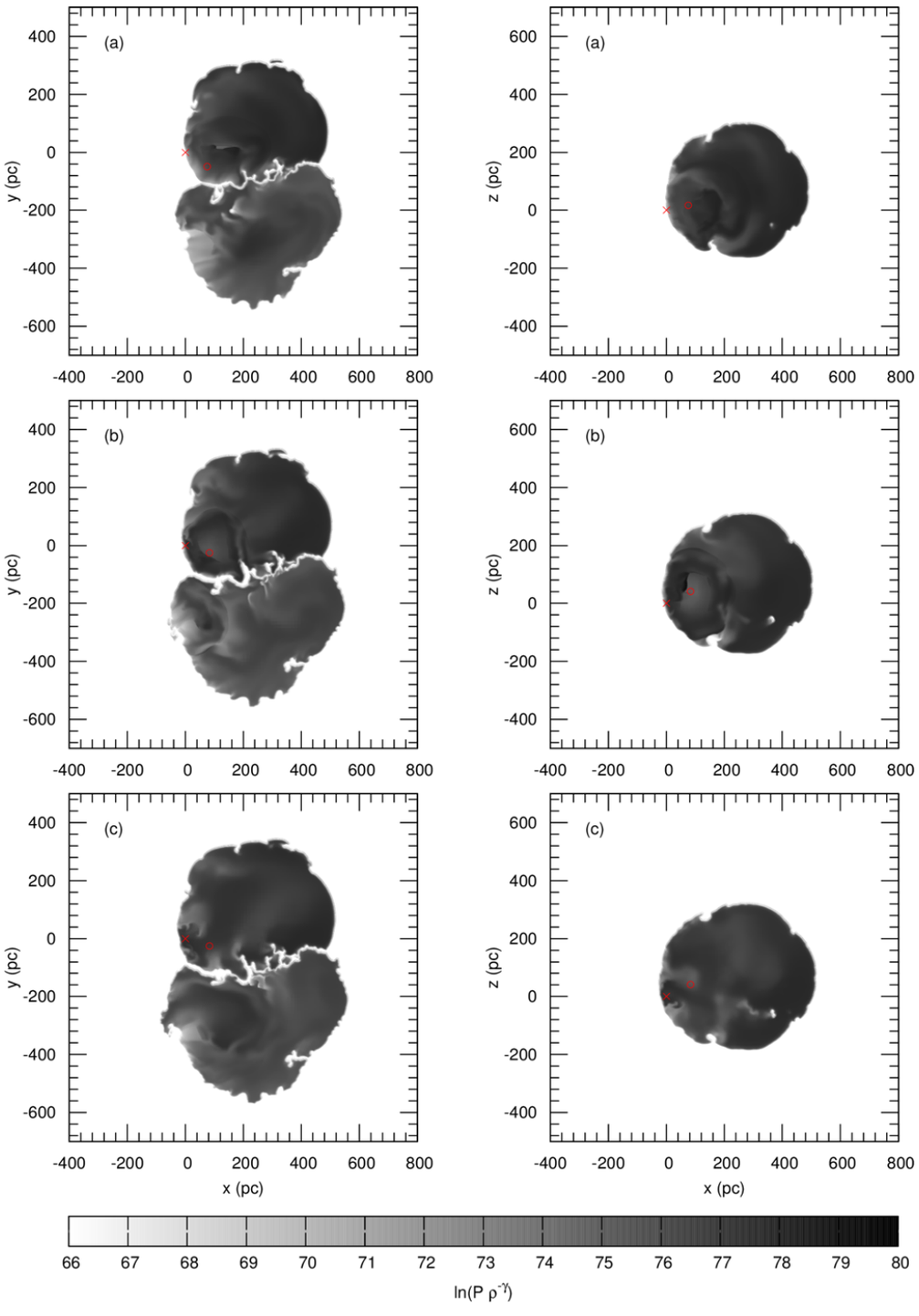

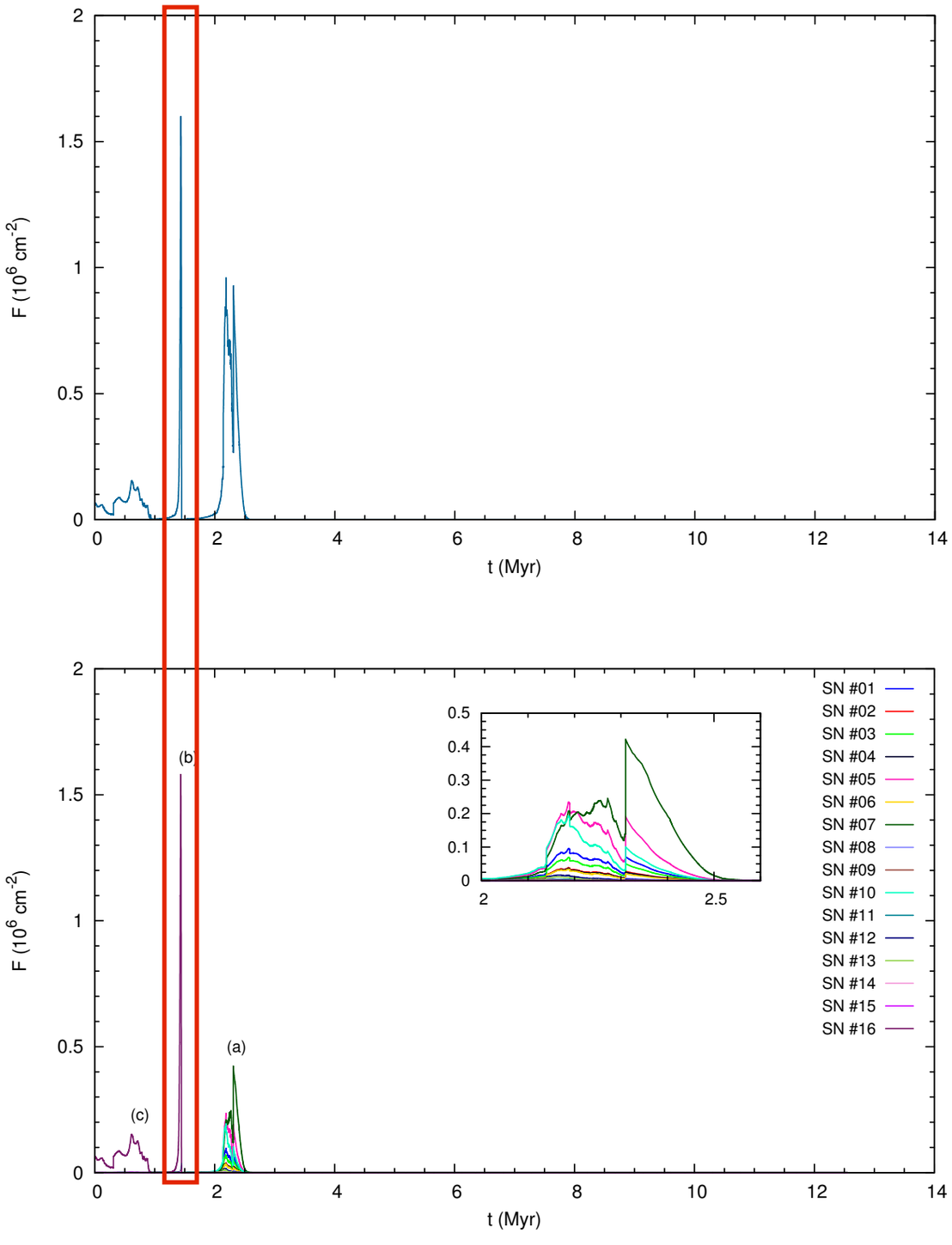

Chemical mixing simulations with homogeneous background medium

Model B: Entropy maps and modeled ^{60}Fe/Fe content in the FeMn crust

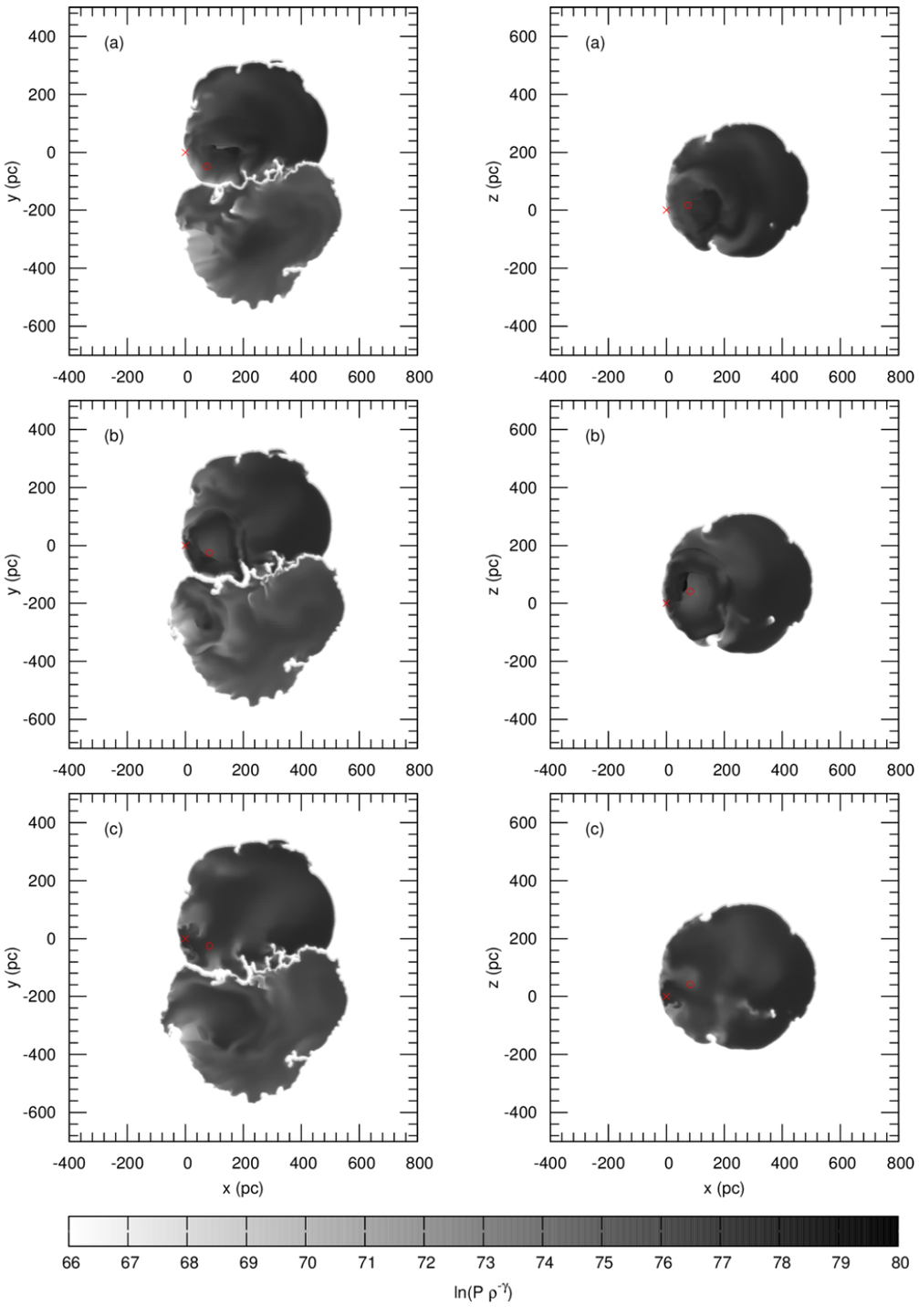

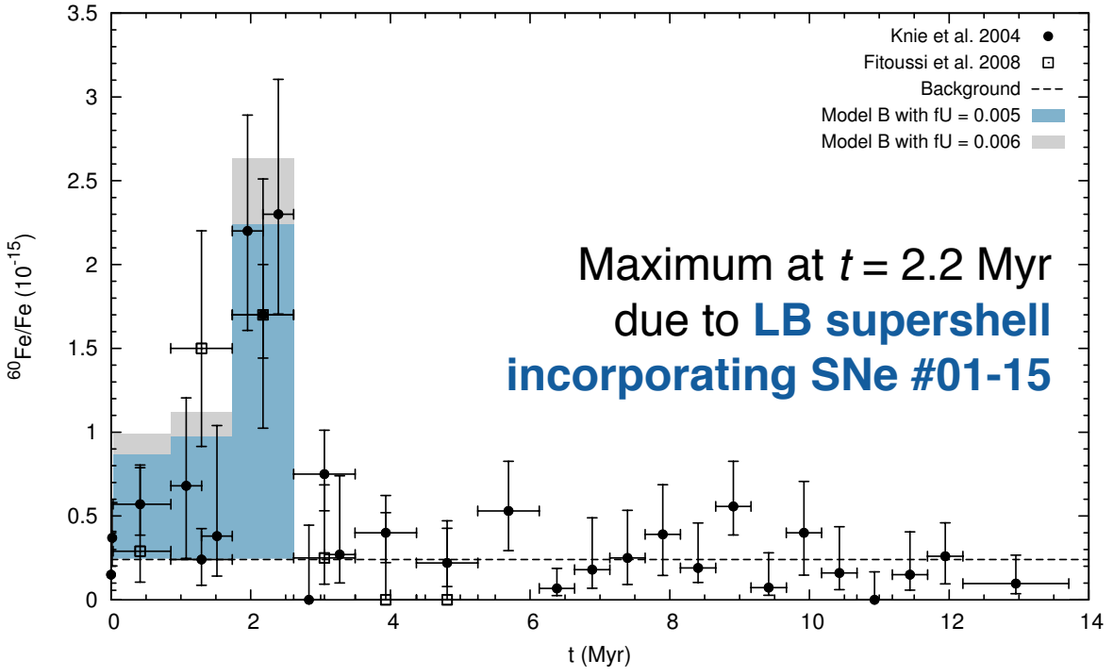

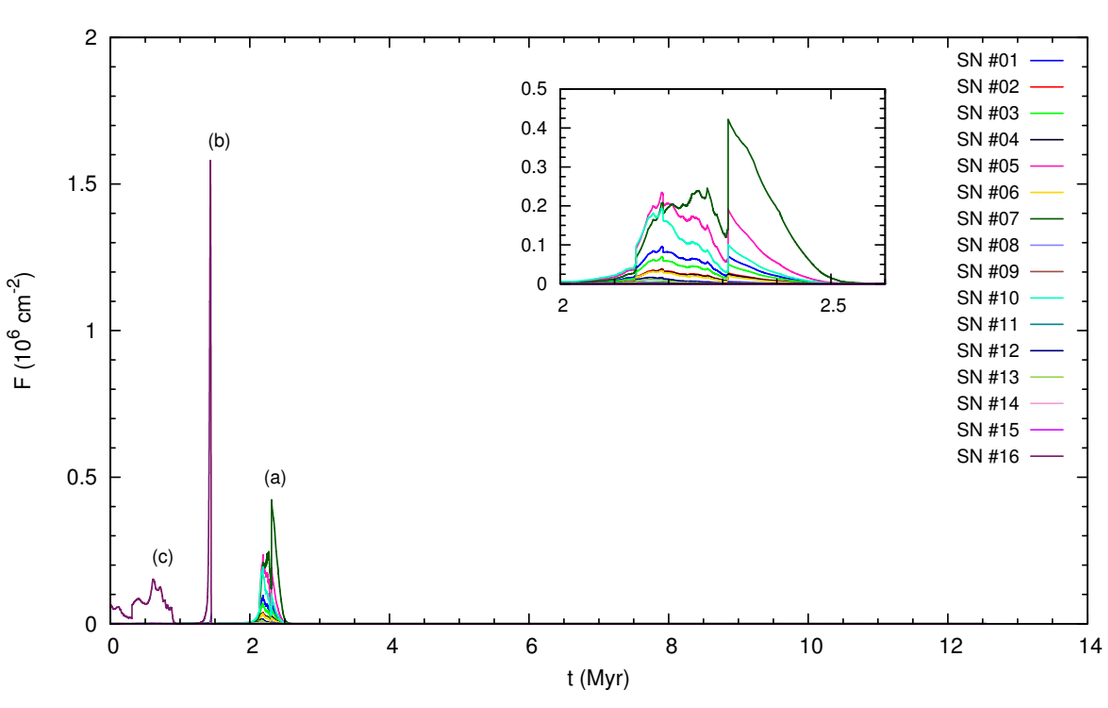

Evolution of the Local Interstellar Medium

Atomic hydrogen number density and gas column density distribution (cuts through z = 0 and y = 0; 180 Myr evol. time)

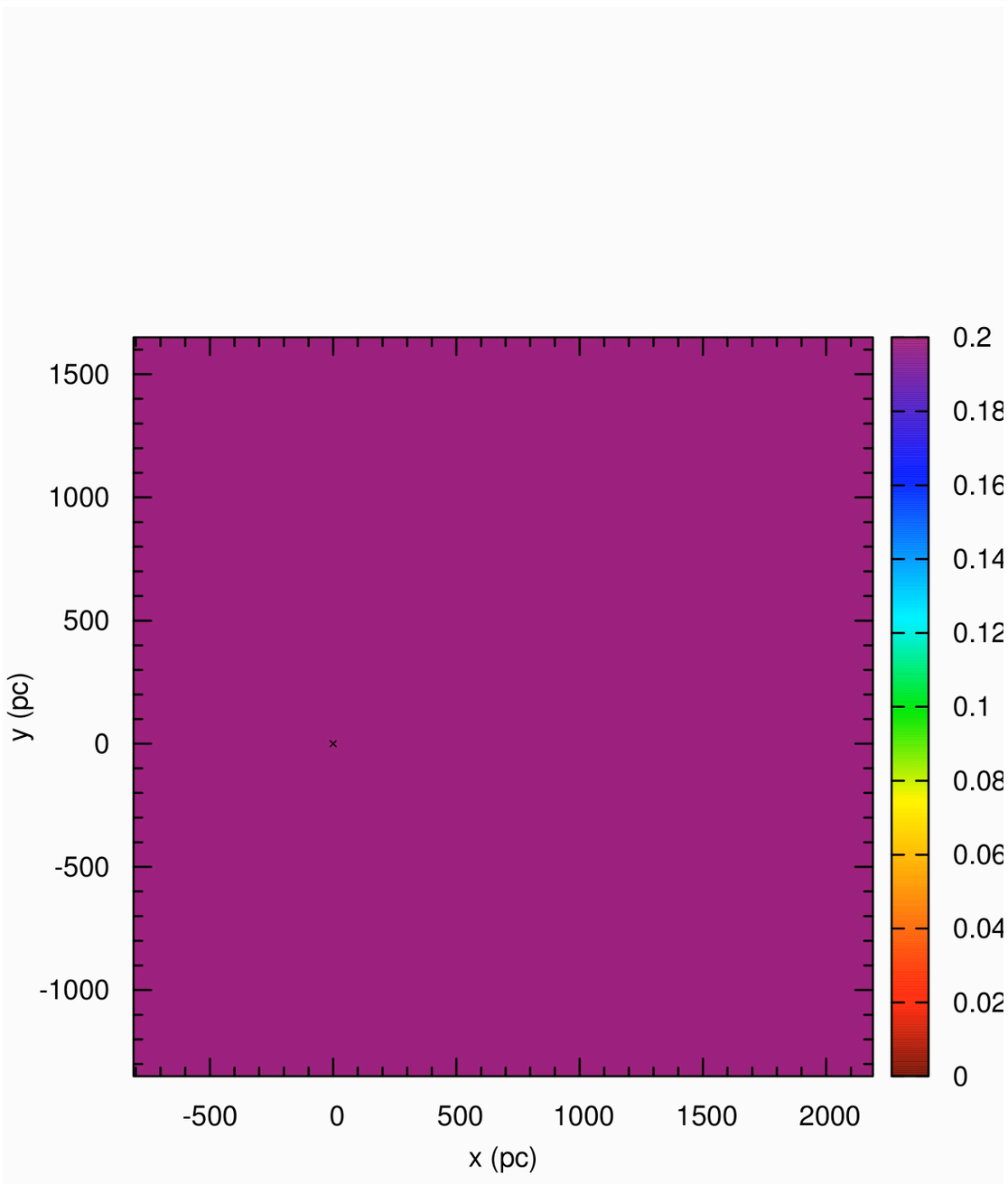

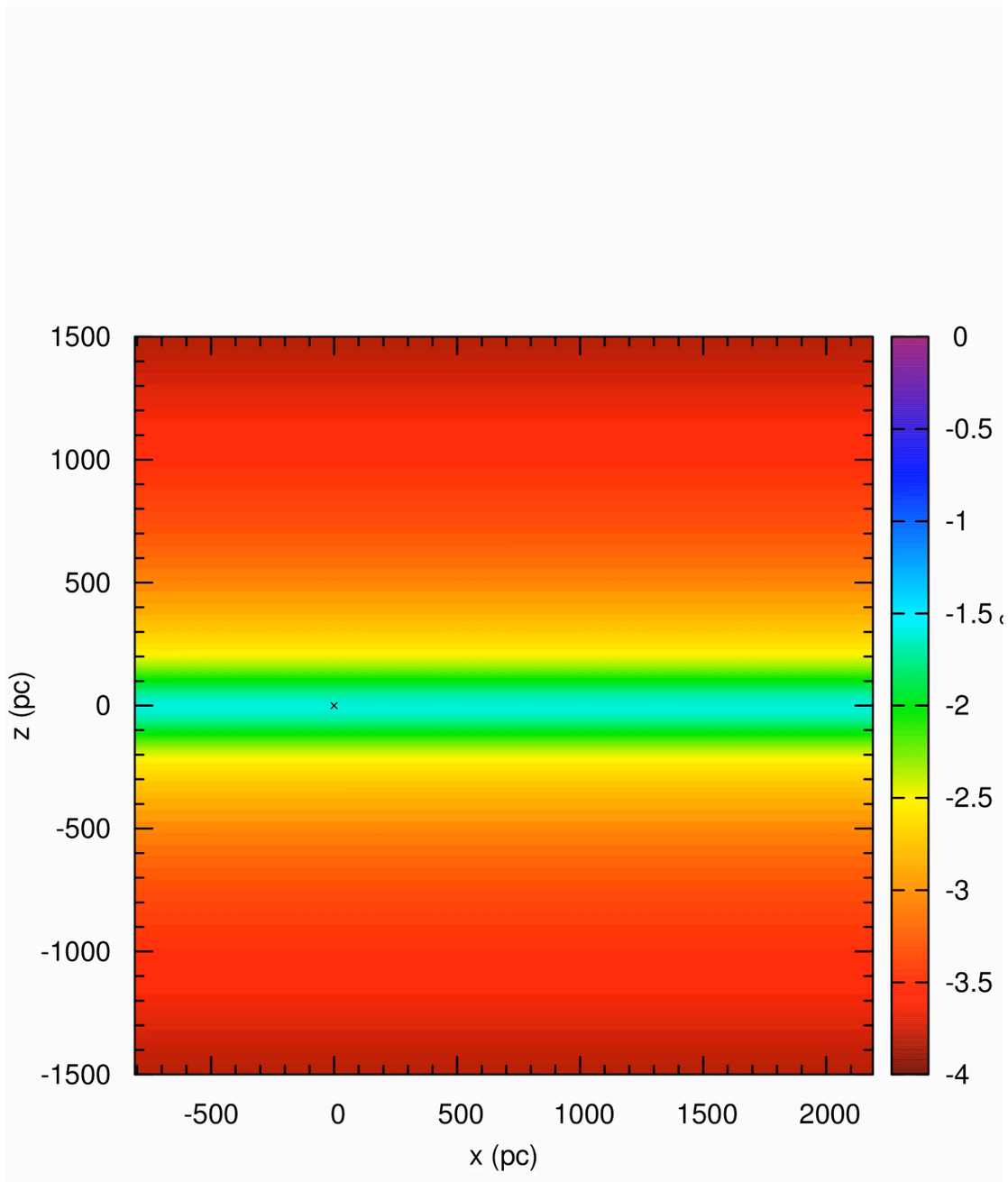

Chemical mixing simulations with inhomogeneous background medium

Model C: Evolution of the atomic hydrogen number density distribution (cuts through $z = 0$ and $y = 0$)

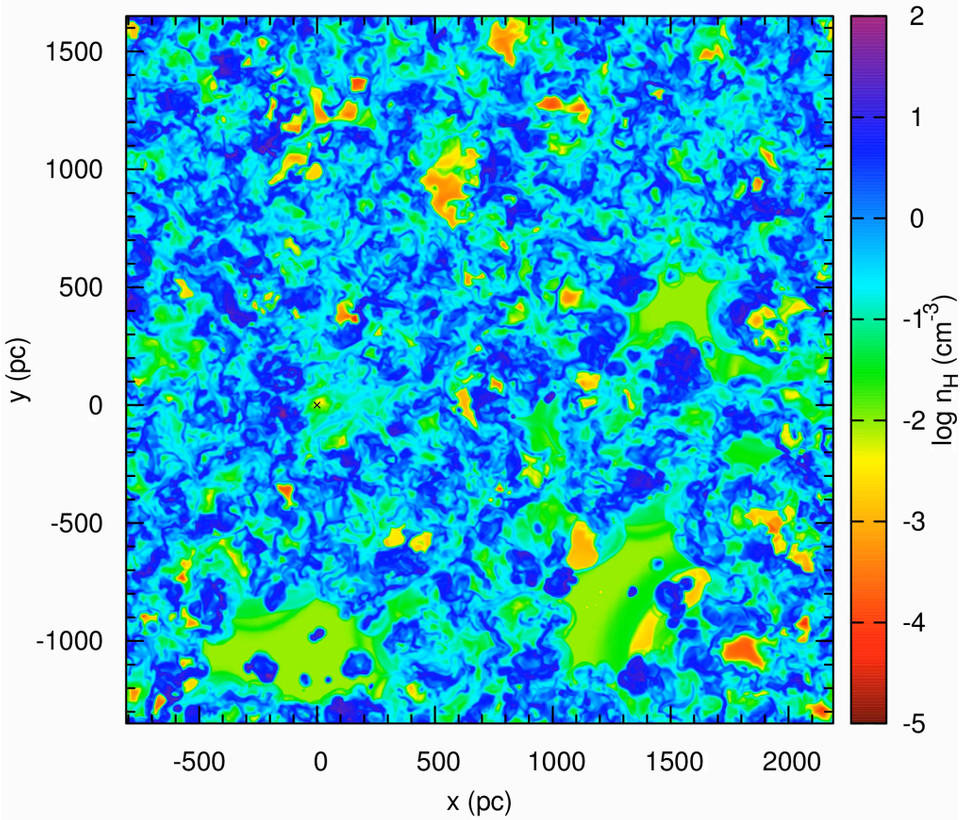

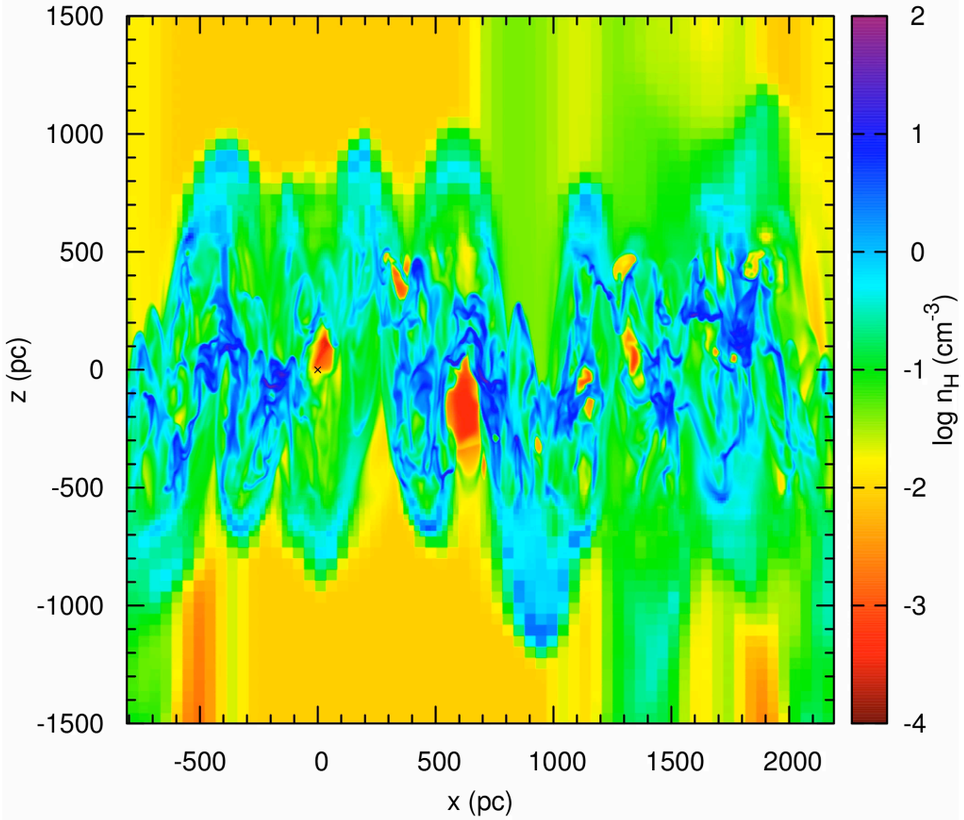

- Launch LB SNe in **"suitable"** environment
- search for extended region that remains sufficiently thin ($n \gtrsim 0.3$ cm^{-3}) at least for a few Myr
- dense gas with enough mass and small flow gradients for cluster star formation

- Internal structures after ~8 Myr due to influence of ambient density/pressure gradients
- 'Present' LB extension: $(x,y) = (280,260)$ pc, $|z| \gtrsim 500$ pc (northern half resembles chimney)
- Hydrogen density and temperature in 'present' LB cavity: $10^{-4.1}$-$10^{-2.2}$ cm^{-3}, $10^{4.5}$-$10^{6.5}$ K

Chemical mixing simulations with inhomogeneous background medium

Model C: Evolution of the ^{60}Fe mass density distribution (cuts through $z = 0$ and $y = 0$)

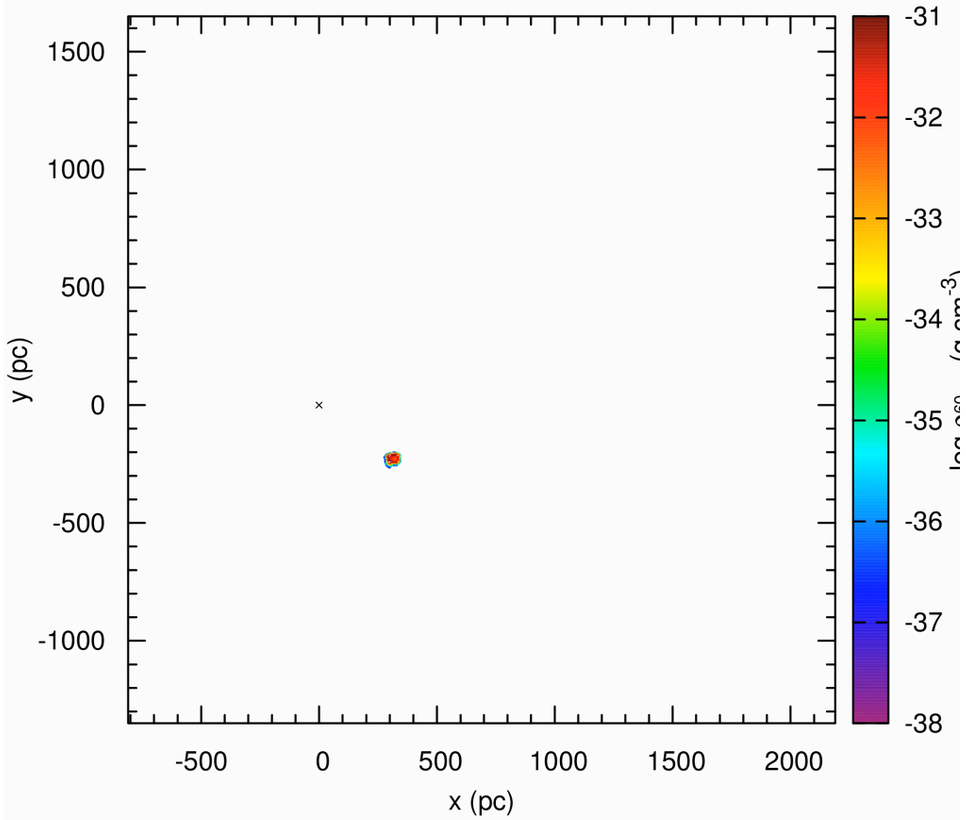

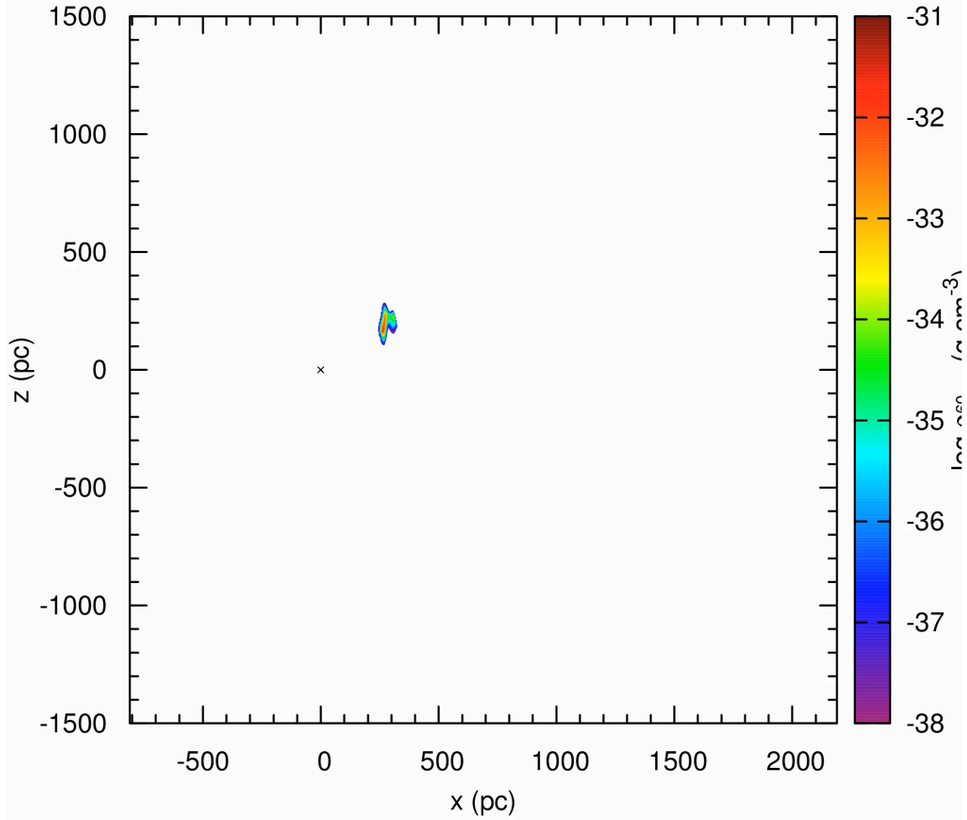

No interstellar ^{60}Fe background → model gives lower limit of ^{60}Fe content in the local ISM!

Chemical mixing simulations with inhomogeneous background medium

Model C: Comparison between models and crust measurements

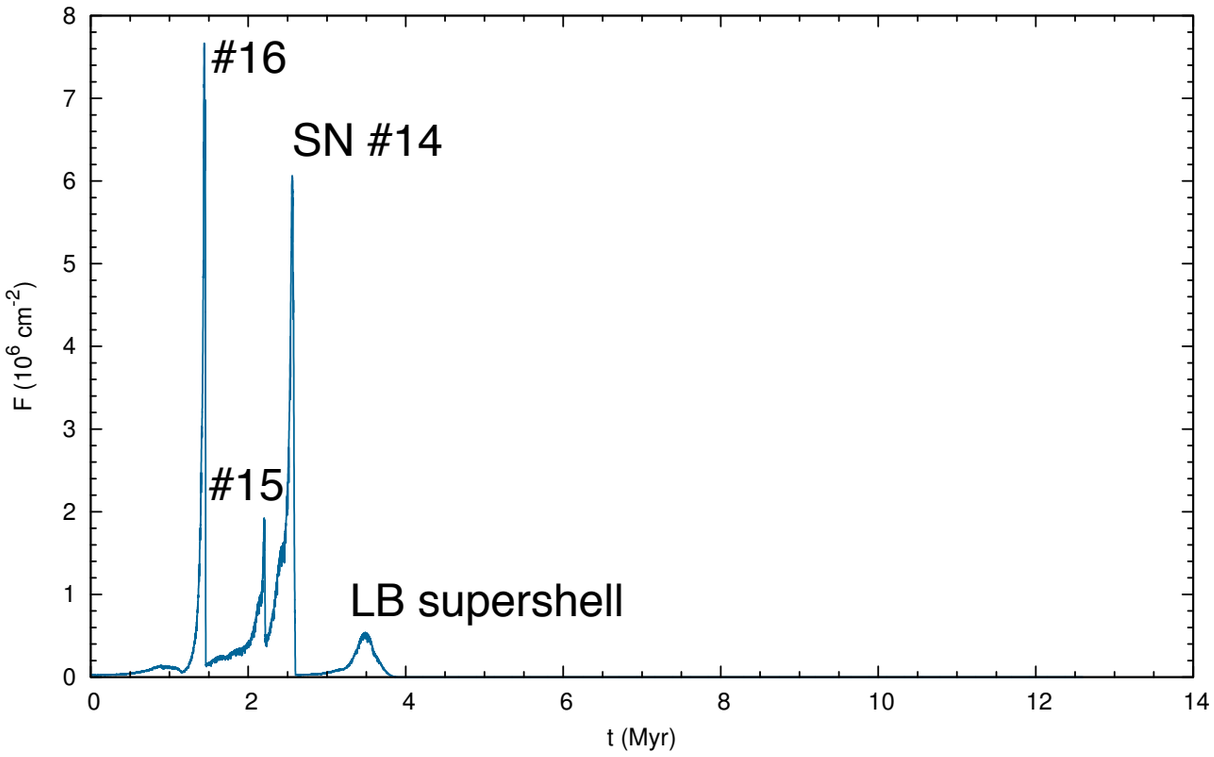

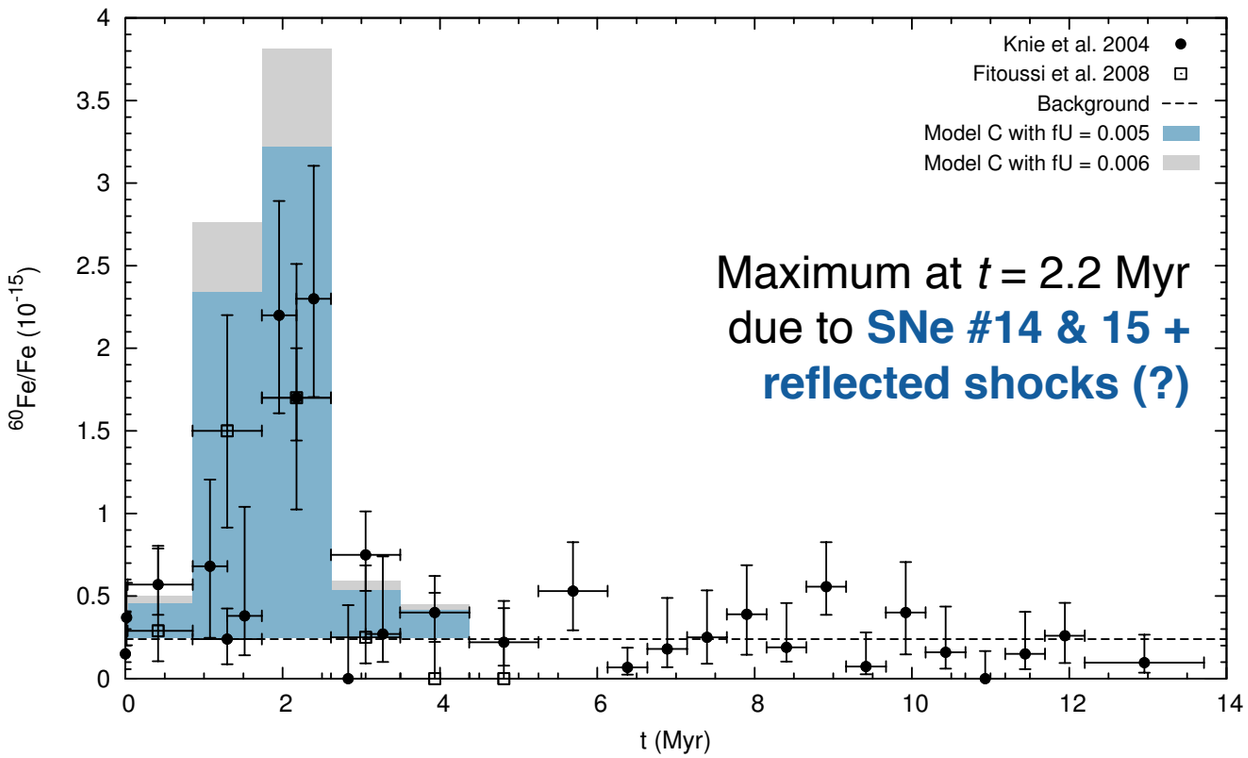

- Artificial signal broadening due to 4x lower resolution
- Model C is a hybrid of model A and B:
  - Fewer pulses due to individual SNe than in model A, but more than in model B
  - Mean density of medium around LB lies in between model A and B [i.e., $(n)_{VA} \simeq 0.2$ cm^{-3}]
  - Supershell arrives later than in A, but earlier than in B → self-gravity unimportant in LB evolution

Comparison of numerical and analytical results

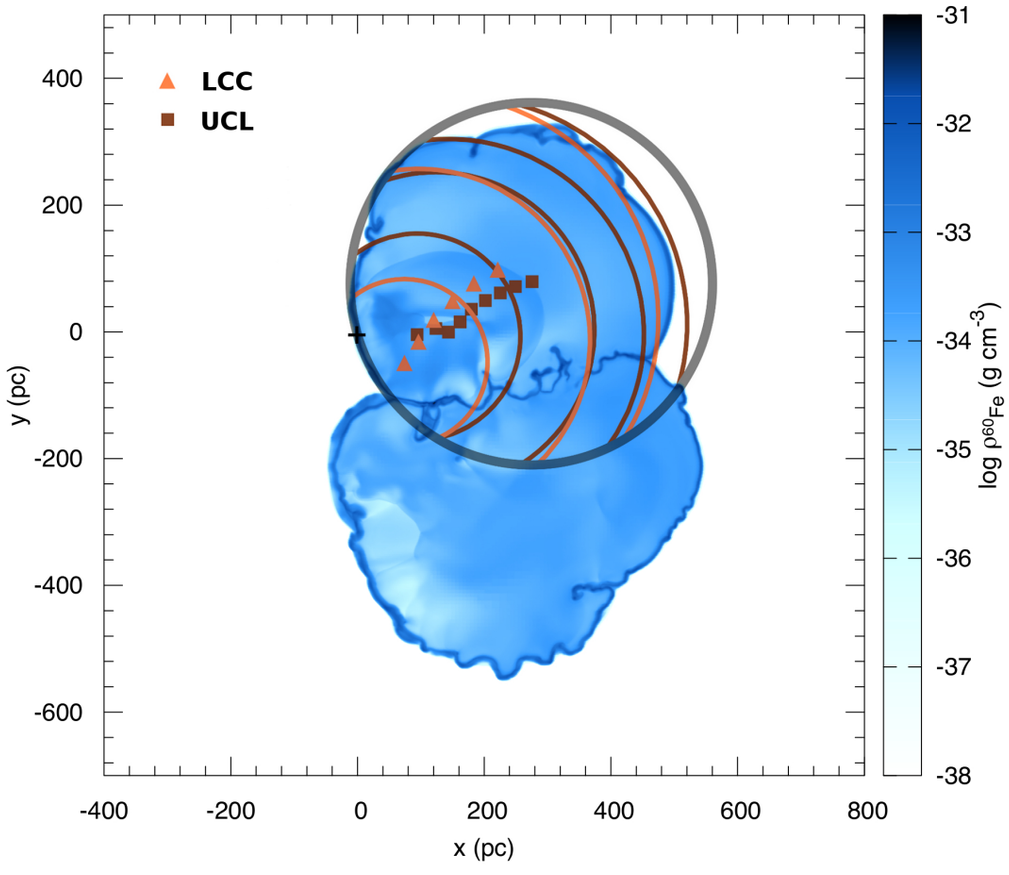

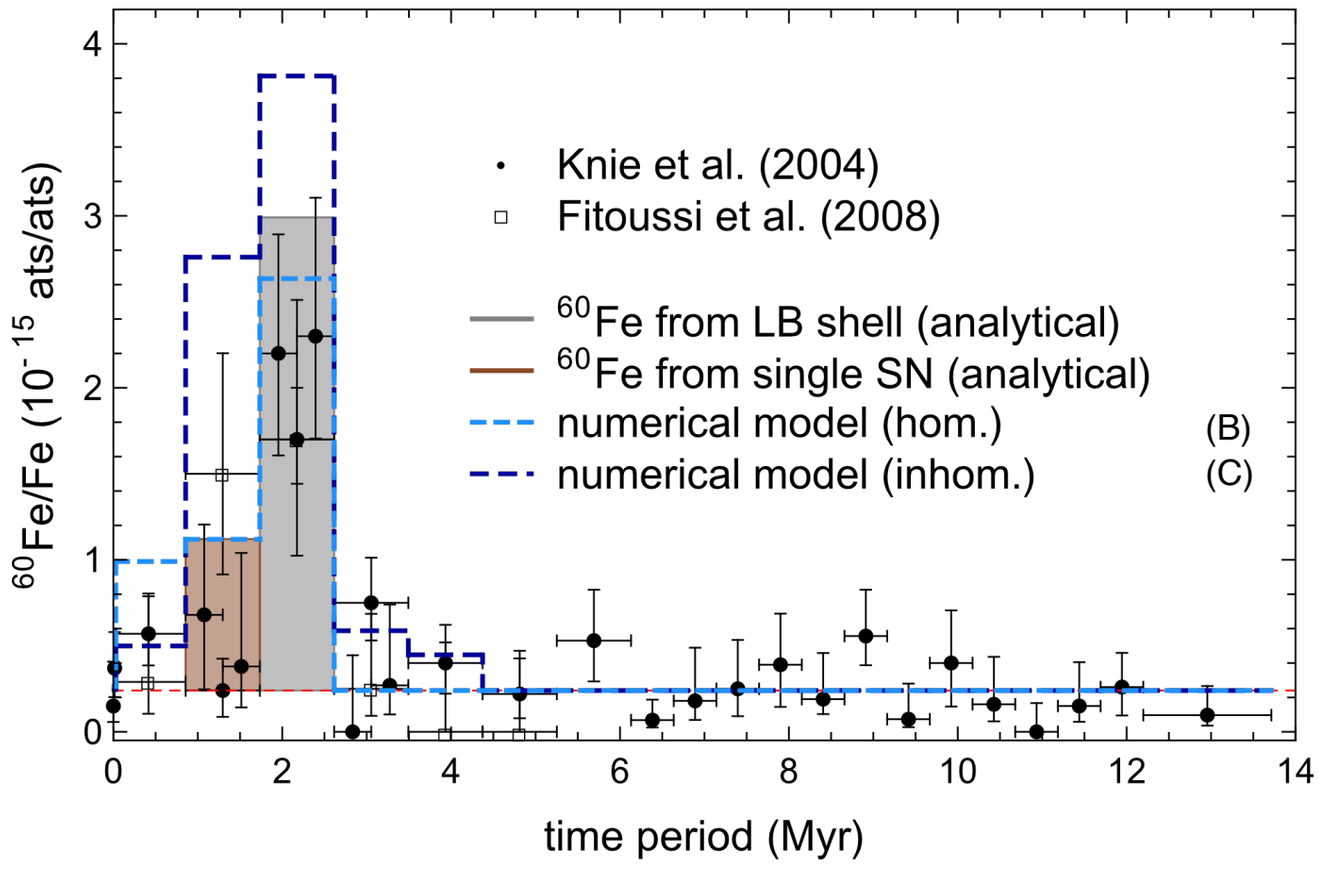

Supportive findings

1) Extended ^{60}Fe peak (1.5-3.2 Myr ago) in deep-sea archives from all major oceans (Wallner+ 2016)

- global phenomenon
- width hints at more than one SN

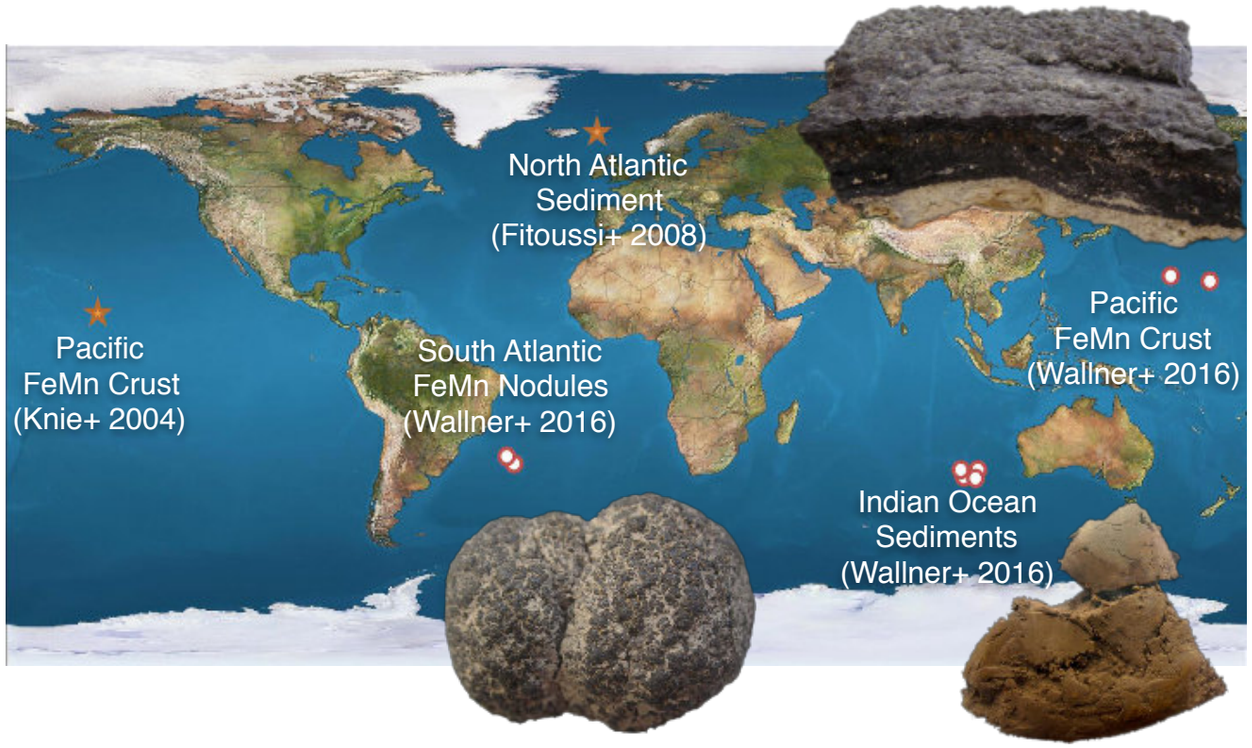

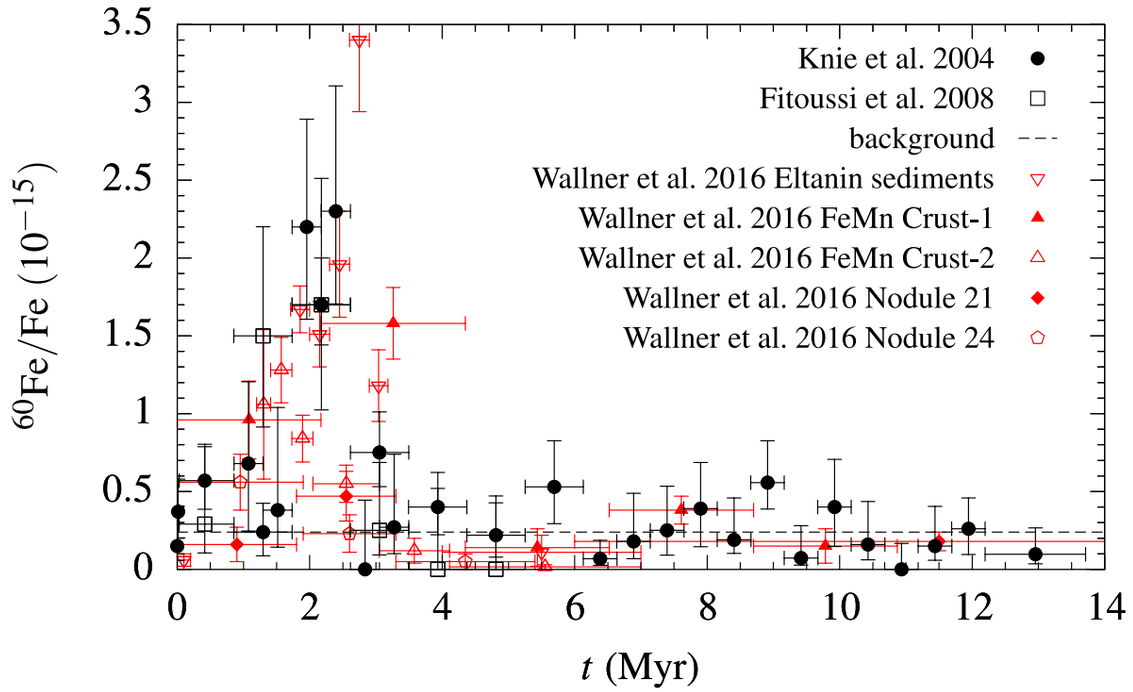

2) Increased ^{60}Fe levels in microfossils dated at 1.8-2.6 Myr (Ludwig+ 2016)

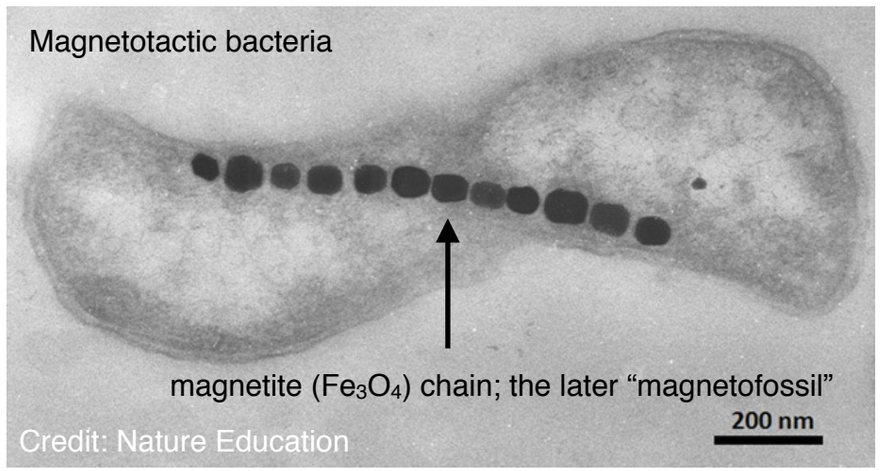

Measurements in two independent Pacific Ocean sediment cores: 42/47 ^{60}Fe events in core A/B

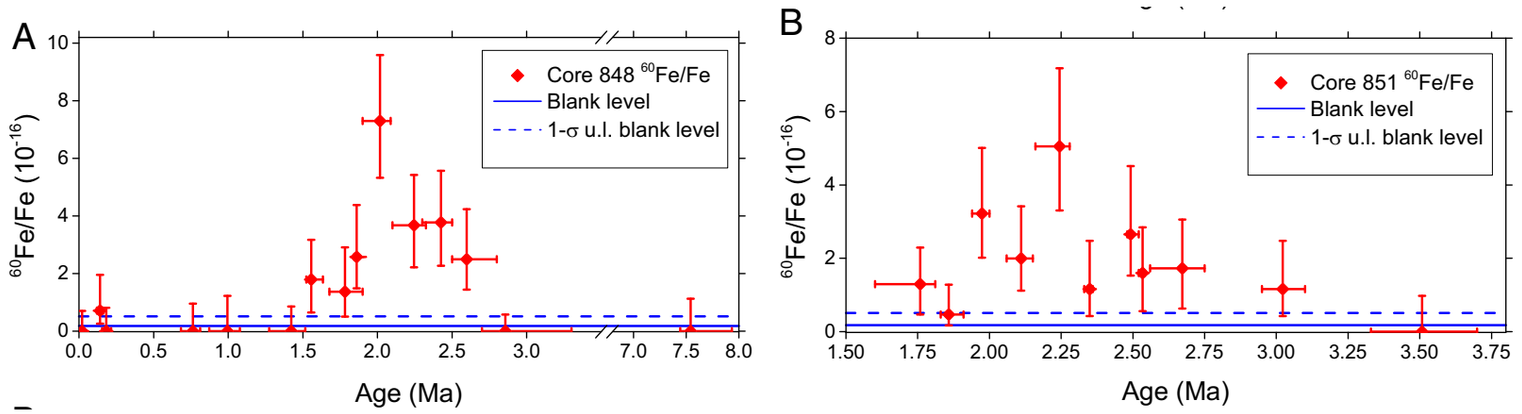

Supportive findings

3) Enhanced ^{60}Fe signatures in lunar soil samples from Apollo 12, 15, and 16 (Fimiani+ 2016)

- No time-resolved measurements due to ‘gardening’ and absence of sedimentation
- Detected integrated fluence ($F \sim 10^7$–6×10^7 cm^{-2}) compatible with LB model if, e.g., $U = 1$, $f = 0.016$

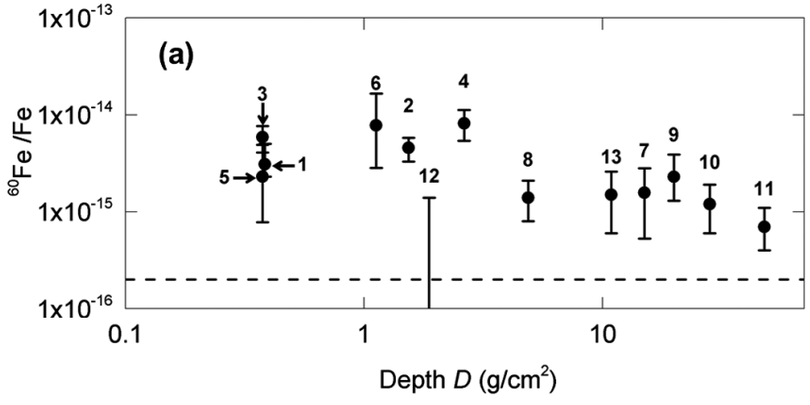

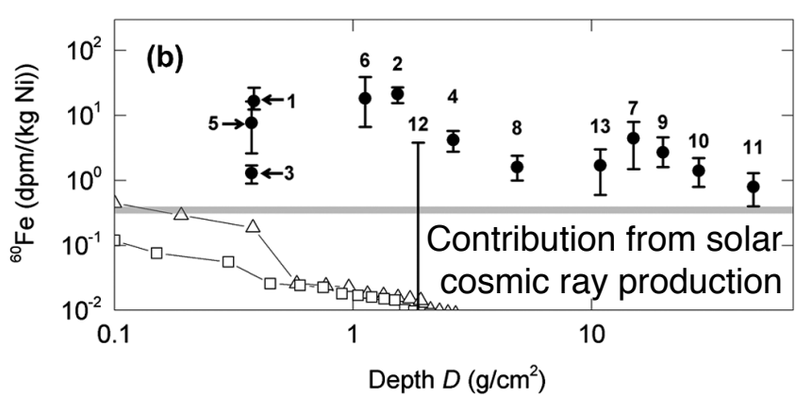

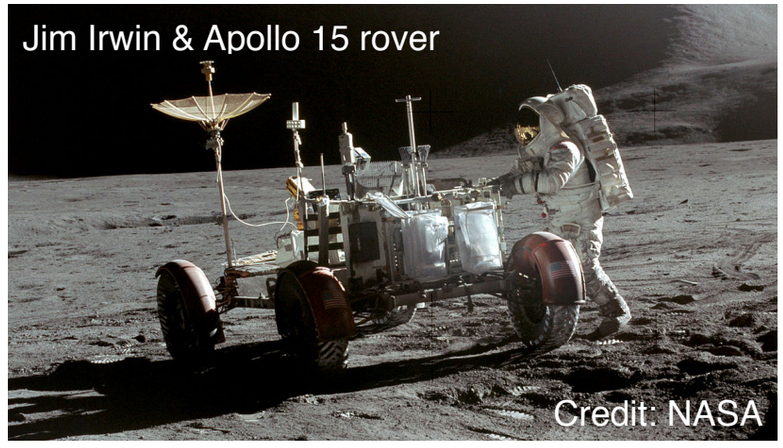

4) Soft X-ray emitting cavities in 3D local interstellar dust maps match estimated sites of the two most recent SNe (Capitanio+ 2017)

- Directions within 3° and 7°, respectively
- Similar distances

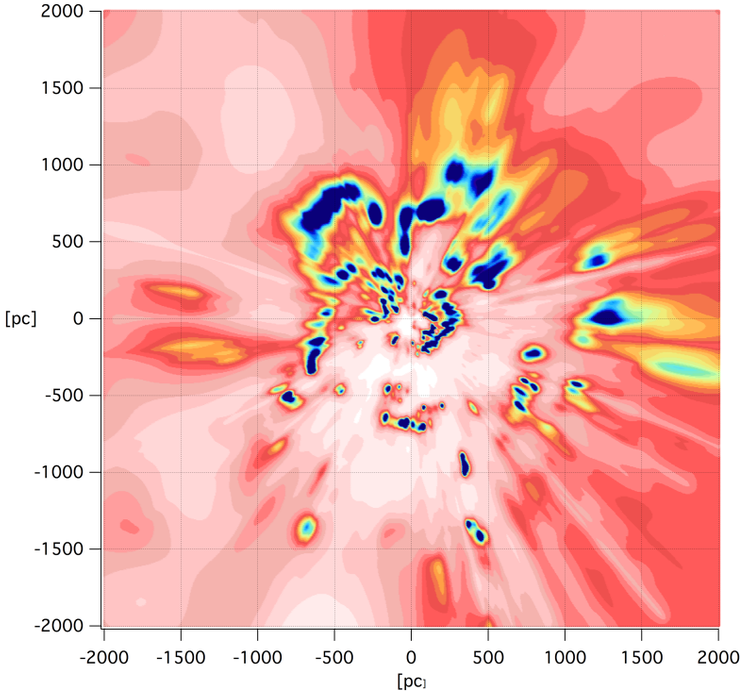

Regions lying in directions of ROSAT 3/4 keV X-ray brightness enhancements (cf. Puspitarini+ 2014)

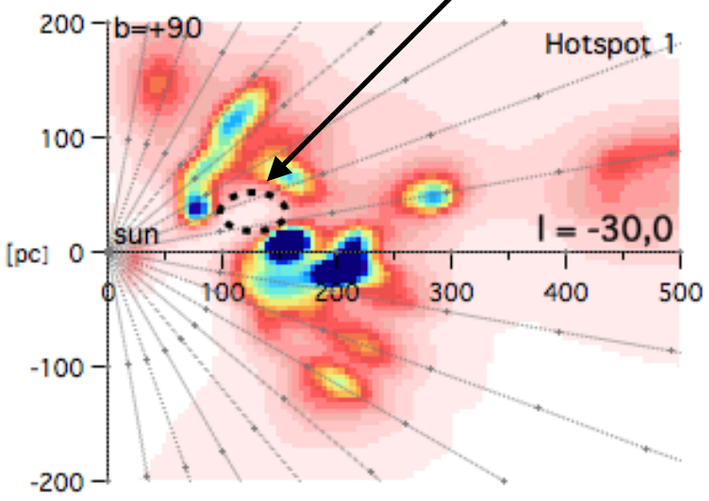

SN #15

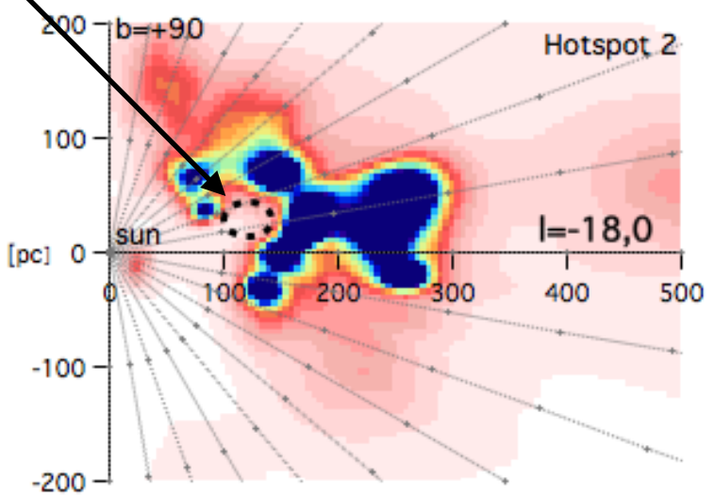

SN #16

Supportive findings

5) Connection to cosmic rays

- During 17 years, ACE-CRIS experiment collected 3.55×10^5 iron nuclei; among them are 15 ^{60}Fe nuclei
- CRIS energy range: ~100–500 MeV/nuc → acceleration of nuclei by SN blast waves (1st order Fermi process)
- ^{60}Fe/^{56}Fe ratio → time elapsed since ejection: a few Myr
- Distance to source from ^{60}Fe half-life: < 620pc (diffusion model!) (Binns+ 2016)
- PAMELA/AMS-02 measured excess of positrons and antiprotons ≥ 20 GeV, plus discrepancy in slope of protons and heavier nuclei → consistent with SN source at ~100 pc distance 2–3 Myr ago (Kachelrieß+ 2015, 2018)
- Yet undiscovered pulsar in LB ($d \sim 30-80$ pc, $\dot{E} \sim 10^{33-34}$ erg s^{-1}) responsible for local high-energy cosmic ray electron spectrum (López-Coto+ 2018)

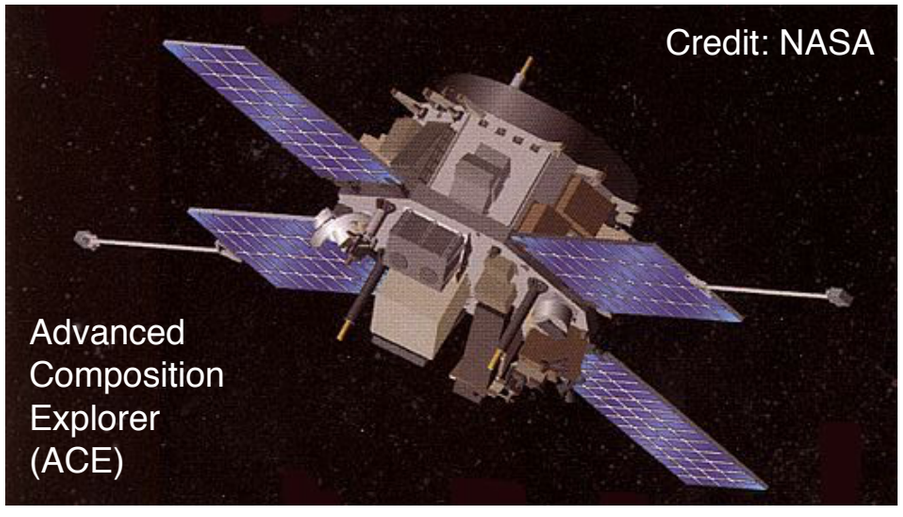

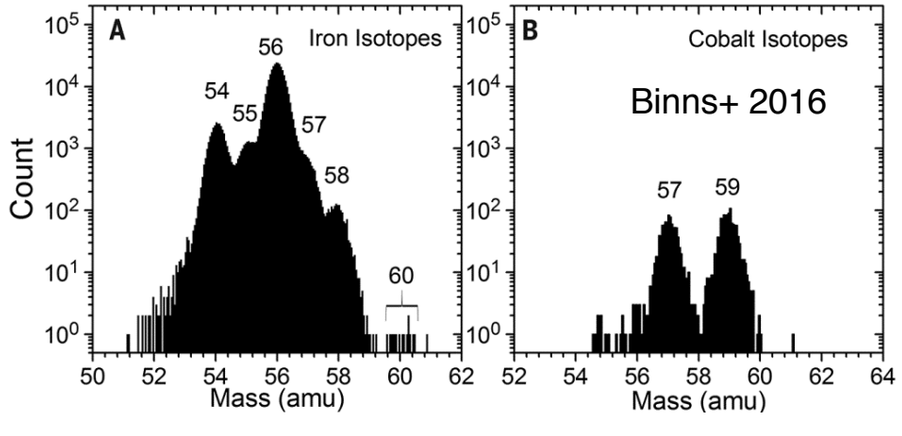

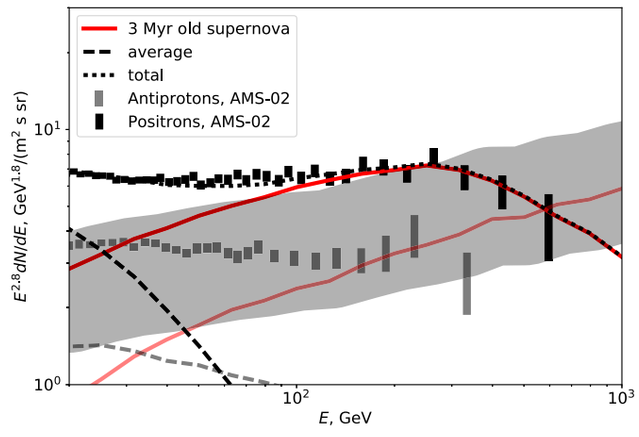

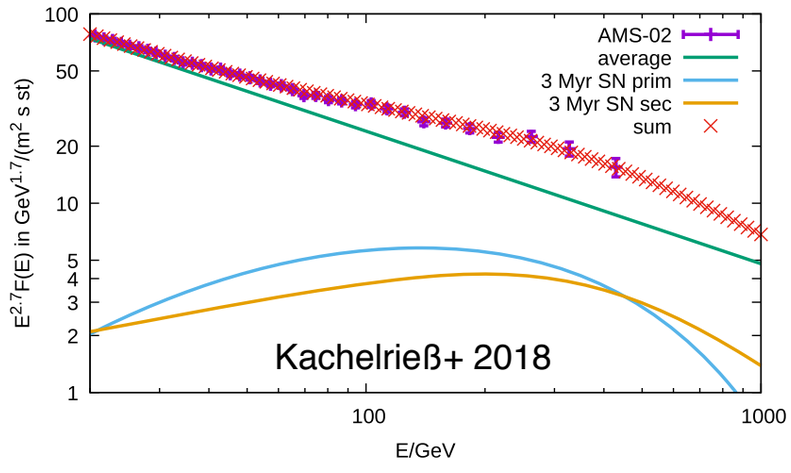

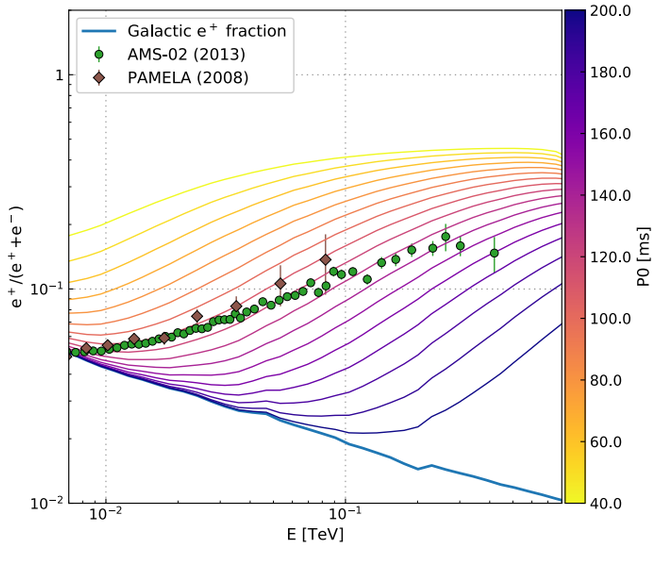

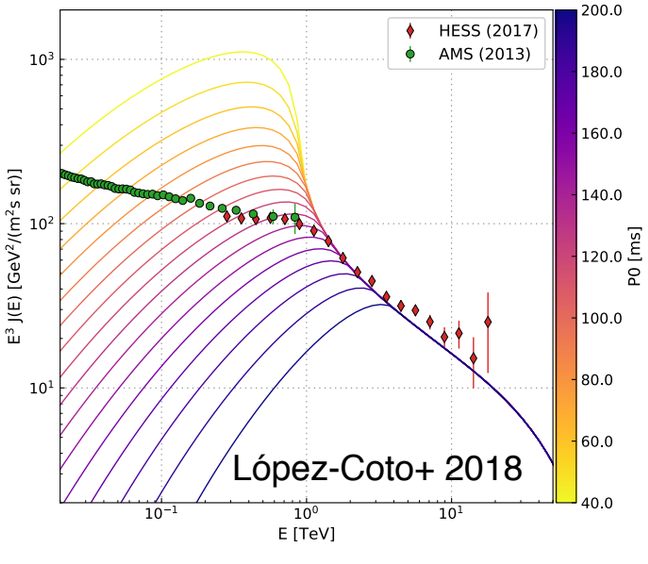

Summary

- **Analytical** and **numerical** computations show that SNe creating the LB can also reproduce ^{60}Fe in the crust
- **Cluster age** derived from stellar isochrones
- **Explosion times** derived from stellar masses
- **Masses** derived from IMF using most probable binning
- **Cluster trajectory** derived from epicyclic eqs. using phase space (**x**-**p**)-coordinates from Hipparcos & ARIVEL data
- **Explosion sites** derived from most probable paths of the perished moving group members
- **^{60}Fe yields** taken from stellar evolution calculations
- **Mixing** with ISM followed via passive scalars
- **Joint evolution** of the Local & Loop I SB studied numerically for 3 models: two homogeneous and one inhomogeneous
- Models **reproduce both the timing and the intensity of the ^{60}Fe excess observed** with rather high precision
- **Two deposition scenarios**:
  - individual fast-paced SNRs, whose blast waves can become reflected from the LB's outer shell,
  - the LB supershell itself injecting ^{60}Fe of all previous SNe over a longer time range
- LB properties observed are best matched by the model with inhomogeneous background medium

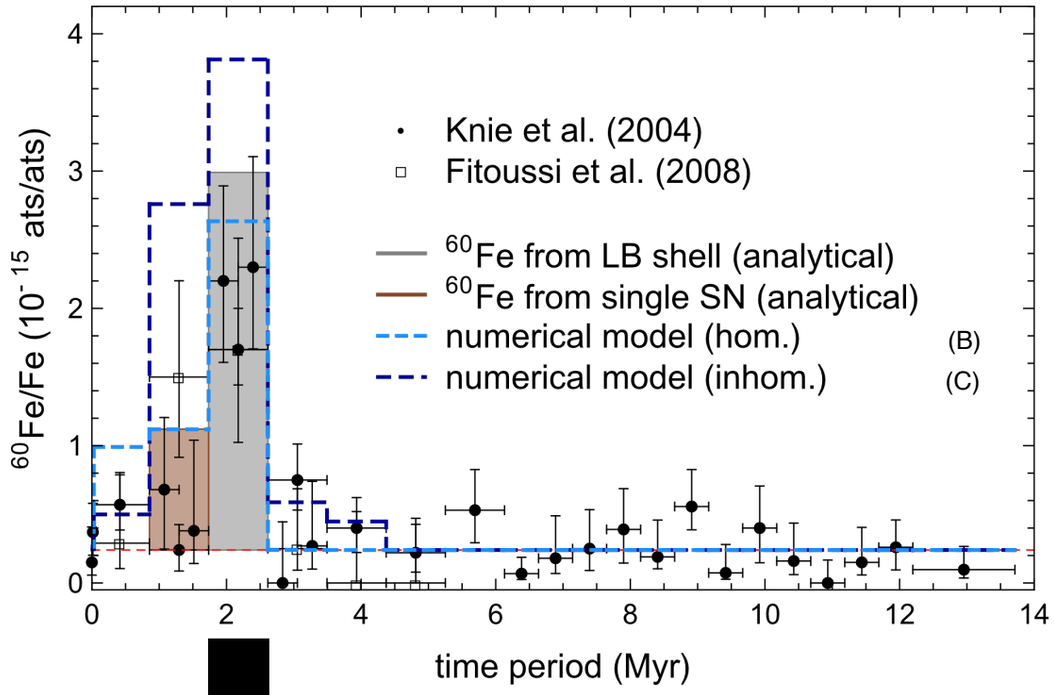

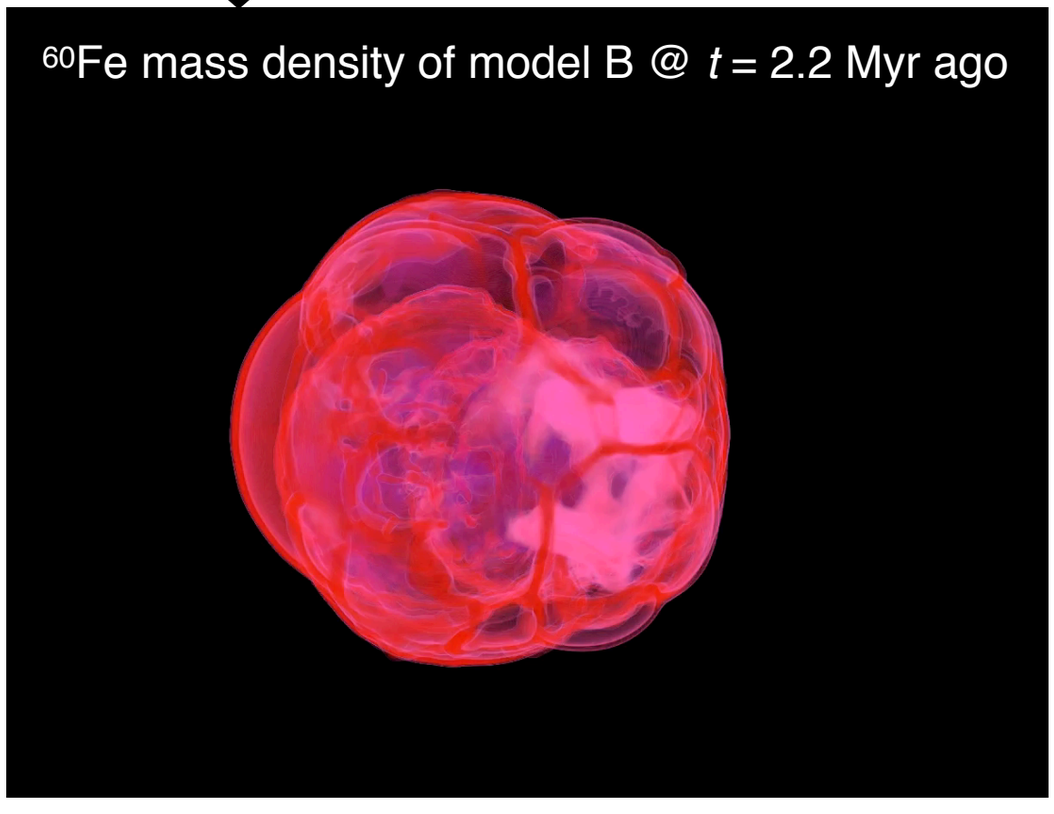

Model uncertainties and potential improvements

General

- Background medium: profound impact on evolution and final dimensions of the SBs
  - Trace back/remodel history of the local ISM using GAIA data
  - Use 3D high-res. reddening maps of the local ISM (Lallement et al. 2018)
    - cloud cavities consistent with last SN explosion centers
    - cannot serve as initial condition for whole LB evolution (> 10 Myr); might only be applicable for last explosion(s)
  - Interstellar magnetic field
- Explosion sequence: left unchanged until now (already includes most probable explosion centers for considered stellar moving group)
  - Refine underlying IMF using Bayesian statistics
  - GAIA data

Radioisotope transport modeling

- ^{60}Fe yields ← stellar evolution models
- Uptake factor ← measurements of ^{60}Fe at other sites or analysis of other radioisotopes
- ^{60}Fe dust survival fraction ← comprehensive description of formation and survival of SN dust at different composition and size
- Additional tracer elements (also for background medium evolution)
- Further ^{60}Fe bump 6.5–8.7 Myr ago (Wallner+ 2016): if related to LB formation (and not due to influx of enriched IDPs or MMs; Farley+ 2006) → Further constraint for our LB formation scenario → clustering of stars between 12 and 15 $M_\odot$ (deviation from most probable mass binning); earlier arrival of LB supershell?

Further reading and other media

- Schulreich, M.M. 2015, Ph.D Thesis, TU Berlin, Germany
- Breitschwerdt, D. *et al.* 2016, Nature, 532, 73
- Feige, J. 2016, Phys. Unserer Zeit, 47, 220
- Feige, J. *et al.* 2017, JPS Conf. Proc., 14, 010304
- Schulreich, M.M. *et al.* 2017, Astron. Astrophys., 604, A81
- Schulreich, M.M. *et al.* 2018, Galaxies, 6, 26

Attack of the stars: Radioactive debris from ancient supernova battered Earth millions of years ago

International Business Times (UK)

Exploding Stars Spat Radioactive Debris All Over Earth

National Geographic

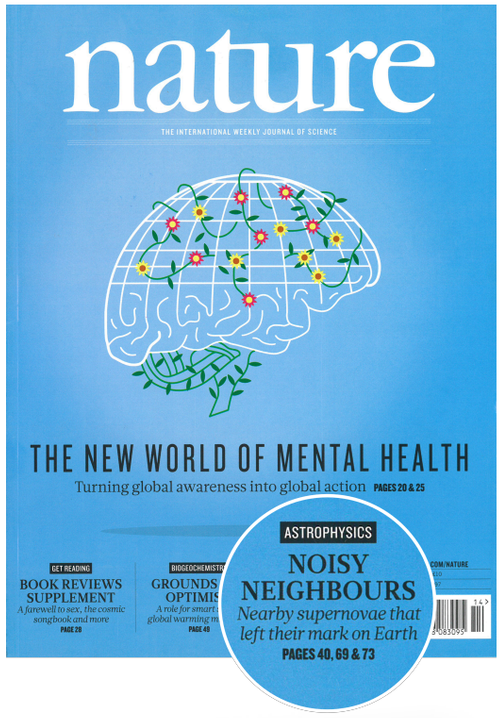

Radioactive material in ocean crusts likely came from nearby star explosions

The Verge

Proof that ancient supernovae zapped Earth sparks hunt for after effects

phys.org

Exploding stars left recent, radioactive mark on Earth

BBC News

Supernova Fallout Hit Earth When Human Ancestors Were Alive

Air & Space

Ancient exploding stars hurled radioactive debris at Earth — and it's still here

Washington Post

How Our Oceans Helped Reveal The Closest And Most Recent Exploding Stars To Earth

Buzzfeed

Finding the Earth-bound evidence for supernovae in the galactic neighbourhood

physicsworld.com

Parameters for Local Bubble supernovae

t_{SN}	m ($M_\odot$)	M_{ej} (10^{-5} $M_\odot$)	x (pc)	y (pc)	z (pc)	D (pc)	l (°)	b (°)	α	δ	sc
-12.6[2]	19.86	6.3	277	75	89	300	15.15	17.23	17^h17^m	$-7°09^m$	Oph
-12.0[3]	18.61	5.5	223	99	71	254	23.94	16.22	17^h37^m	$-0°21^m$	Oph
-11.3[2]	17.34	5.0	251	67	87	274	14.95	18.52	17^h12^m	$-6°39^m$	Oph
-10.0[2]	15.41	4.2	227	57	83	248	14.10	19.53	17^h07^m	$-6°48^m$	Oph
-10.0[3]	15.36	4.1	185	77	67	211	22.60	18.49	17^h27^m	$-0°23^m$	Oph
-8.7[2]	13.89	3.6	203	45	79	222	12.50	20.80	17^h00^m	$-7°23^m$	Oph
-8.0[3]	13.12	3.4	151	49	57	169	17.98	19.75	17^h14^m	$-3°34^m$	Oph
-7.5[2]	12.65	3.3	181	31	75	198	9.72	22.22	16^h49^m	$-8°46^m$	Oph
-6.3[2]	11.62	3.0	163	11	73	179	3.86	24.10	16^h30^m	$-12°03^m$	Oph
-6.1[3]	11.48	2.9	121	19	47	131	8.92	20.99	16^h52^m	$-10°04^m$	Oph
-5.0[2]	10.76	2.7	145	-5	69	161	-1.97	25.43	16^h12^m	$-15°19^m$	Sco
-4.2[3]	10.21	2.6	97	-15	33	104	-8.79	18.58	16^h16^m	$-24°35^m$	Sco
-3.8[2]	10.02	2.6	125	1	51	135	0.46	22.19	16^h28^m	$-15°40^m$	Oph
-2.6[2]	9.37	2.4	95	-9	47	106	-5.41	26.22	16^h01^m	$-17°05^m$	Lib
-2.3[3]	9.21	2.4	75	-49	17	91	-33.16	10.74	15^h10^m	$-45°35^m$	Lup
-1.5[2]	8.81	2.3	83	-25	41	96	-16.76	25.31	15^h32^m	$-24°44^m$	Lib